Low Fluence Neutron Radiography Techniques

by

Dennis William Klein

Submitted to the Department of Nuclear Engineering in partial fulfillment of the requirements for the degree of

Master of Science

at the

Massachusetts Institute of Technology

January, 1997

Author .....
Department of Nuclear Engineering
January 17, 1997

Certified by .....
Richard Lanza
Principal Research Scientist
Thesis Supervisor

Read by .....
Lawrence Lidsky
Professor of Nuclear Engineering
Thesis Reader

Accepted by .....
Jeffrey Freidberg
Chairman, Departmental Committee on Graduate Students

Low Fluence Neutron Radiography Techniques

by
Dennis William Klein

Submitted to the Department of Nuclear Engineering on January 17, 1997, in partial fulfillment of the requirements for the degree of Master of Science

Abstract

This research developed a quantum limited neutron detector with high spatial resolution utilizing Charge Coupled Device (CCD) technology for neutron radiography based on a low fluence accelerator neutron source. Our primary concern was the non-destructive testing (NDT) of Aluminum (Al) for hidden corrosion by detection of Aluminum Hydroxide ($Al(OH)_3$). By a detailed signal and noise analysis of CCD based imaging systems, a CCD based quantum limited detectors was designed and tested.

A counting circuit was found to be the most effective means of developing a quantum limited system. One counting circuit that was developed involved a simple thresholding technique based on a fast frame rate, low noise (or intensified) CCD camera. The second counting circuit utilized a series of computational filters and algorithms to recover neutron events from a fast frame rate, low noise CCD. The parameters for using both have been evaluated. The largest limitations of counting circuits for practical applications are the high cost of fast frame rate CCDs and the high cost of Digital Signal Processing (DSP) boards required to process the information. This is not a limitation for low neutron fluences, due to the development of low cost video frame rate CCDs and low cost Personal Computers (PCs) which are currently capable of simple signal processing at video frame rates. Furthermore, the developing technology for lower cost, higher frame rate CCDs and low cost, more capable PCS will eventually eliminate these limitations completely.

An unexpected result of this research was the suitability of a CCD based counting circuit as a high spatial resolution neutron counting device for non-imaging applications such as neutron scattering experiments.

A number of techniques were investigated to maximize the detected neutron fluence. A more powerful accelerator source was suggested. It was recommended that the beam energy be increased from 900 keV to 1100 keV to take advantage of the increased low energy neutron production in the $^{9}Be(d,n)^{10}B$ reaction. A better moderator and collimator design was investigated and a technique was developed for future optimization based on MCNP trials. Finally the efficiency of the Li^{6}-ZnS neutron detector scintillator screen was improved.

Thesis Supervisor: Richard Lanza
Title: Principal Research Scientist

Acknowledgments

I would like to thank those people who have made this work possible. Financial support for this work was provided by grants from the United States Air Force Office of Scientific Research (FA49620-93-1-0291 DEF), and the Federal Aviation Administration (FAA Grant 93-G-053), and the Navy, who employed me while I pursued this work.

Dr. Richard Lanza was an energetic source of ideas and advice. I would like to thank him for his moments of inspiration and his ability to modestly point out solutions to problems that hindered my project. I would like to thank Dr. Lawrence Lidsky for his advice in the compilation of this work.

This project was greatly aided by advice of Dr. Erik Iverson. I would also like to thank Marc Berte for his contributions. This project would not have been possible without the help of Jennifer Walsh, Mike Timmons, Mark Van Der Helm, Todd Pleune, Mike McMahon, and all of the people at Catholic Fellowship, who helped me develop and maintain a healthy perspective on research.

Finally, I would like to thank my parents, William and Victoria Klein, for their unconditional love and support. They have shown me that all things are possible through God.

Table of Contents

List of Figures

1. Introduction

1.1. Goal of This Thesis

The goal of this research was to further the development of a mobile neutron radiography system for detection of hidden corrosion in aircraft components.

1.2. Main Contributions of This Thesis

A quantum limited, high spatial resolution, low fluence neutron detection system was designed and developed using a CCD camera. The parameters and limitations for its use have been evaluated. Its application for imaging and non-imaging systems was explored.

This thesis also made recommendations for changes to the experimental setup to maximize the detected neutron fluence from our accelerator source.

1.3. Outline of Thesis

Part I is dedicated to describing the background behind need for a mobile, capable neutron imaging system. A general discussion of nuclear imaging techniques is introduced.

In Part II, our experimental setup is described and each component's contribution to the overall signal and noise is described.

In Part III, the optimization of our system takes place in three parts- first, optimizing the signal to noise of our system to develop a quantum limited system. Second, the design and implementation of a counting circuit are demonstrated. Finally, the system is optimized by increasing the detected neutron fluence. There is a discussion of the findings and implications of this work.

2. Application Driven Research

This research was initiated to investigate methods for non-destructive detection of corrosion in aircraft.

2.1. Problem Statement

Corrosion in aircraft frames is most severe near rivet joints in aluminum parts. The mechanism which initiates failure is most usually pitting and/or hydrogen embrittlement. These forms of localized corrosion are difficult to detect because affected areas can be quite small, and are usually hidden inside metal to metal joints. Once initiated, localized corrosion can proceed at a much higher rate of metal loss than generalized corrosion, leading to premature failure of the aircraft. For these reasons, hidden, localized corrosion is difficult to detect, and even more difficult to predict.

If a non-destructive method of detection of hidden corrosion existed, the aircraft industry would be able to more reliably determine the health of their aging aircraft, and more easily prevent catastrophic in-flight failure. The result would be a dramatic savings in preventative maintenance to their aircraft, the life of their aircraft, and most importantly, the safety of passengers and crew members.

2.2. Design Constraints

The aircraft industry requires a non-destructive detection of corrosion in aircraft that meets several criteria. First, it must be of a reasonable cost to build and operate to make it a feasible and attractive option. It must be capable of penetrating the metal skin of the aircraft, while being able to detect micron thicknesses of corrosion. It should be portable enough to fit into existing hanger facilities. Finally it should be pose no health threat to the workers or the general public. These criteria are outlined in Figure 2.1.

Detection System Criteria:
- Sensitive to Micron Thickness Corrosion
- Penetrate Metal Skin
- Reasonably Low Cost
- Minimal Health Risk
- Portability

Figure 2.1: Criteria for Corrosion Detection System

Section 1: Background Information

3. Imaging Techniques: Radiation Sources

There are a large number of different nuclear imaging techniques that might be used to solve the problem of imaging hidden corrosion inside of the metallic skin of an aircraft. This chapter explains the advantages of using thermal neutron radiography as a solution. The aluminum skin is the substrate material within which we wish to image hidden corrosion. Our project is based on the selective attenuation of neutrons by corrosion.

Three different imaging principles were considered for this project: selective emission, selective reflection, and selective attenuation of radiation. The first principle, selective emission of radiation, would require the phantom material to selectively emit a type of radiation different than the substrate material. Selective radiation can be passive as in infra-red light emission, or induced by an external source of radiation. For example, a neutron or gamma ray capture nuclear reaction often releases secondary radiation. The secondary radiation emission can then be used as the signal for imaging.

Selective reflection could be also used detect materials. Neutron and gamma radiation will be scattered differently by different materials. It would be possible to image a material by designing an experiment which uses the scattered radiation as a signal.

Selective attenuation takes place by a combination of either by selective absorption and scattering of radiation. Radiation is directed onto an object, and the amount of radiation that passes through the object is used as the signal for imaging. The incident radiation that did not survive is said to be attenuated. It should be noted that the signal may contain noise from multiple scatters. This phenomena is known as buildup.

The type of signal that could be used varies greatly. For example, radiation such as charged particles, electro-magnetic field radiation, neutron radiation, magnetic fields, or even non-nuclear techniques such as, ultrasonic vibration and eddy-current measurements could be considered.

3.1. Selecting a Nuclear Imaging Technique to be Used

We have a number of criteria for selecting the optimal imaging technique for a given application. A technique must be selected such that it produces a detectable signal which is strong enough to image the phantom within the substrate material. One of the largest problems is finding a technique that is capable of penetrating the substrate material. Another challenging issue is that the imaging technique must show a large enough difference in the strength or type of interactions between the substrate and the phantom material that it can be used for imaging.

Our solution was to choose a selective attenuation technique. Charged particle beams would not be feasible due to the fact that they would be stopped very quickly by the substrate material. The proper energy neutral radiation beam, such as gamma radiation or neutron radiation, would easily be capable of penetrating our substrate, the metallic aluminum skin of the aircraft.

While considering the type of radiation or field used, we must consider whether we can produce an adequate source strength for our needs. To create a field or source of radiation that

meets our needs, the type of field or radiation that can be produced might require modification before use. For example, we can produce a strong source of multi-energetic neutrons, but the energy spectrum of the neutrons may need to be changed to a relatively mono-energetic source before we can use it. Finally, we must be able to detect the signal which is given off as a result of interacting with this field.

The next requirement is that the intrusive field or radiation must be capable of producing a strong enough differential signal between the corrosion and the substrate which penetrates the substrate material and can be sensed by our detectors. For example, in our system, the neutron beam is attenuated by the substrate ($e^{-\mu X}$). If the substrate material attenuates a very large percentage of our neutron beam, then substantially more beam is required for a reasonable signal to noise. To illustrate, if we consider a substrate material which is a 6" thick plate of aluminum, 40% of a thermal neutron beam would be attenuated as it traveled through the material.

Finally, the intrusive field or radiation must show a high difference in interaction between the substrate and the corrosion. For example, x-rays and energetic gamma rays can penetrate thick layers of aluminum. Both are attenuated more strongly by dense, or high atomic number materials. Therefore, both would be attenuated more by the Aluminum then they would for aluminum hydroxide, $AL(OH)_3$, and the difference signal would produce an image. However, the neutron beam attenuation difference between an aluminum substrate and an aluminum hydroxide phantom is much more significant. For example, attenuation of a 2 mm thick layer of aluminum hydroxide is the same (40% loss of the neutron beam) as the 6 inch thick plate of aluminum. It is also possible that the interaction with the interrogating field or the radiation cause a secondary field or radiation to be emitted differently from the phantom than from the substrate material. For example, selective neutron activation of the phantom may result in gamma rays being given off which can then be imaged.

3.2. X-Ray Radiography

X-ray radiation is used commonly in medical and industrial applications to image hidden materials. This technique requires an x-ray source and an x-ray detector. The image that is formed at the detector relies on selective attenuation of low energy photons by the hidden material. Attenuation of x-rays is strongly dependent on the atomic number of the attenuating material. Behind areas where the beam is attenuated strongly, less x-rays will be collected, and a negative image (the dense materials are shown by light areas while the background is dark) of the phantom is formed. The mass attenuation coefficients for Al, H and O are shown on the following page:

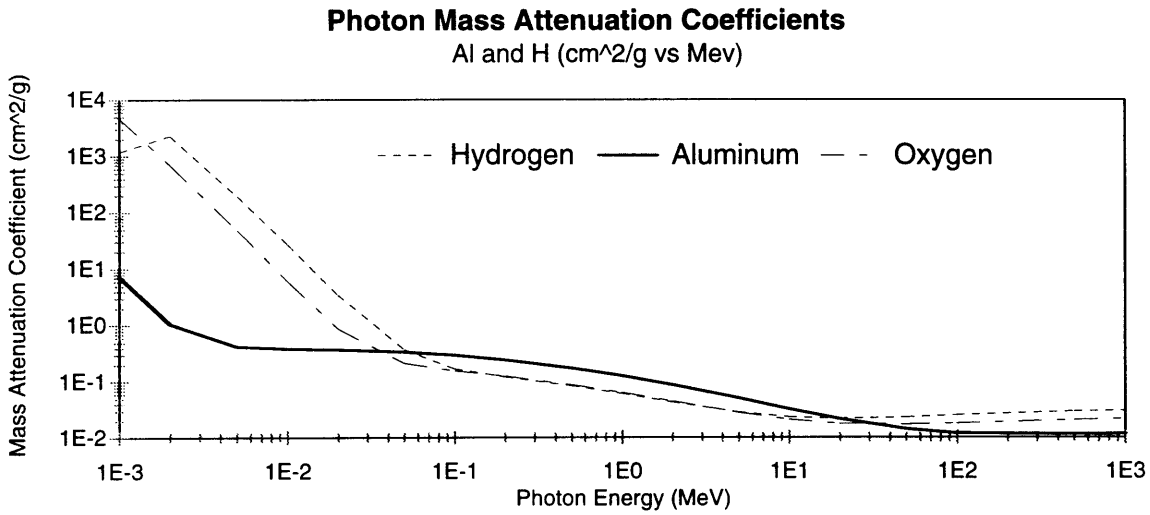

Figure 3.1: Mass Attenuation Coefficients of Hydrogen, Oxygen and Aluminum

It should be noted that the attenuation of an x-ray beam is also a function of the energy of the x-rays. Lower energy x-rays are attenuated much more strongly than high energy x-rays. More significantly, at lower x-ray energies, there is a larger difference between in the attenuation of the x-rays by lower atomic weight materials and the attenuation by higher atomic weight materials. Thus, low energy x-ray beams show a better contrast between different atomic weight materials. However, if the energy selection of the x-ray is too low, the beam may not penetrate the phantom and no object will be formed.

3.3. Reactor Based Neutron Radiography

Neutron radiography, like x-ray radiography, relies on the selective attenuation of a neutron beam from a neutron source-- in this case a fission reactor-- by the material to be imaged. The attenuation of neutrons is a very strong function of the atomic constituents of the material as well as the energy of the neutron beam. Each type of atom and isotope has a unique energy dependence for both absorption and scattering of a neutron beam. If the likelihood, or cross-section, of attenuation for aluminum, oxygen, and hydrogen are shown on the following page.

Aluminum has very large peaks between 1 keV and 1 MeV. Oxygen has similar peaks between 100 keV and 100 MeV. These are known as resonance peaks. At low energies, many materials see an increase in neutron absorption, known as a 1/V dependence, as shown by both oxygen and aluminum. Unlike the resonance peaks, these are large, sustained increases in the total cross section.

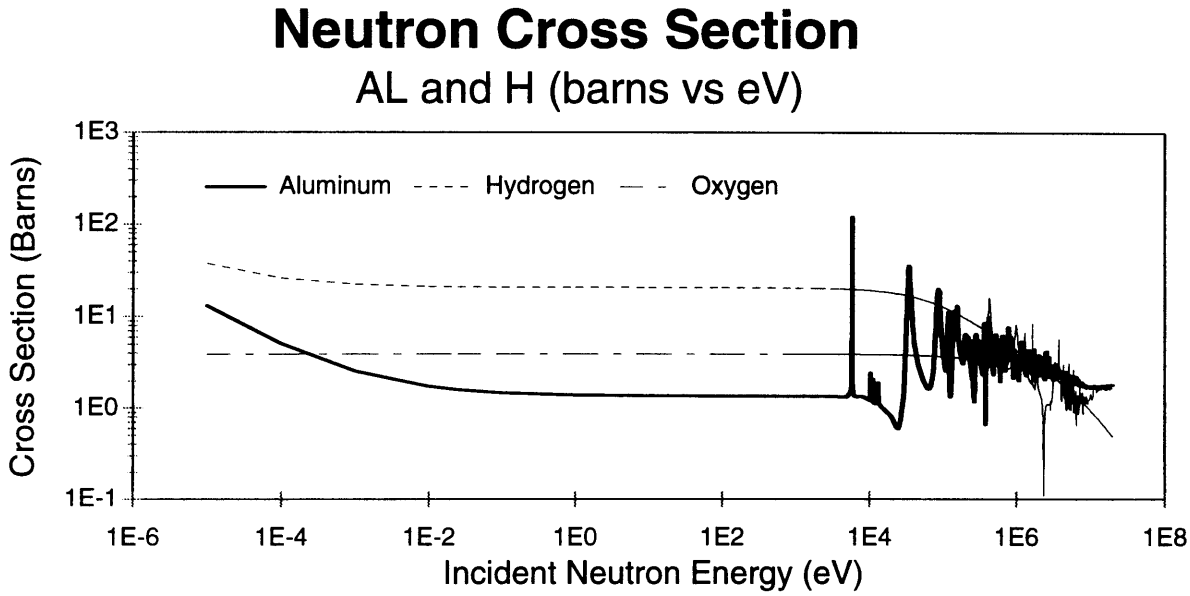

Figure 3.2: Total Neutron Cross-Section (ENDF IV) Curves for Hydrogen, Oxygen, and Aluminum

A fission reactor will create a spectrum of neutrons. By moderation, it is easy to obtain a large number of neutrons with a thermal energy of 2.5 x 10^{-2} eV, which corresponds to room temperature kinetic energy. At this energy, it is interesting to note that hydrogen has a cross section about 20 times larger than aluminum. It should also be noted that other materials such as Boron-10 and Cadmium both show large resonances at this temperature.

To compare the x-ray radiography with neutron radiography, it is necessary to convert both neutron cross-sections and photon mass attenuation coefficients to a more useful form. Attenuation can be expressed in terms of a linear attenuation coefficient (μ) by the following relationship:

$$I(x) = I_O \, e^{\mu x} \tag{3.1}$$

<u>*WHERE*</u>: I = *Intesity of Neutron or X-ray Beam*
μ = *Linear Attenuation Coefficient*
x = *Thickness of Material*

The linear attenuation coefficient for neutrons is:

$$\mu = \frac{\sigma \, \rho \, A}{m_A} \tag{3.2}$$

The linear attenuation coefficient for gamma rays is:

$$\mu = \mu_M \rho \tag{3.3}$$

<u>*WHERE*</u>: M = *Mass Attentuation Ceofficient*
ρ = *Density of Material*
σ = *Total Neutron Cross-Section*
A = *Avagadro's Number*
m_A = *Atomic Mass*

Using these equations, the attenuation coefficient for $Al(OH)_3$ was calculated and graphed for both the gamma ray spectrum and the neutron spectrums. The results are shown on the following page.

As will be discussed in much greater detail, these graphs give us critical information about our system. First, it is desired that we have a large contrast between the substrate (Al) and the corrosion product we wish to detect ($Al(OH)_3$). There is clearly a much larger contrast between low energy neutrons than there is for any regime in the gamma spectrum. Second, it is desired that we be able to penetrate the substrate (Al) of a thickness of at least a centimeter. Therefore it is impractical for the linear attenuation coefficient for Al to be much above 3, ruling out the use of low energy gamma rays. From the graph, it is evident that gamma rays below 100 keV would not penetrate the substrate material.

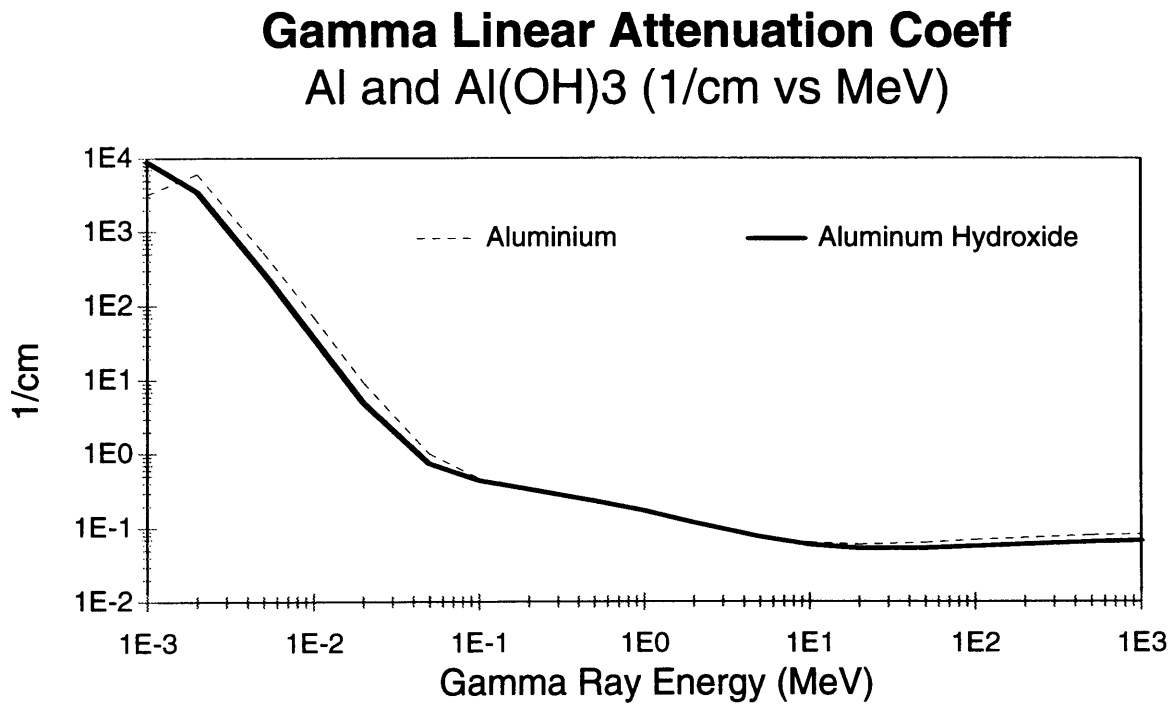

Figure 3.3: Gamma Ray-- Linear Attenuation Coefficients for Al and $Al(OH)_3$

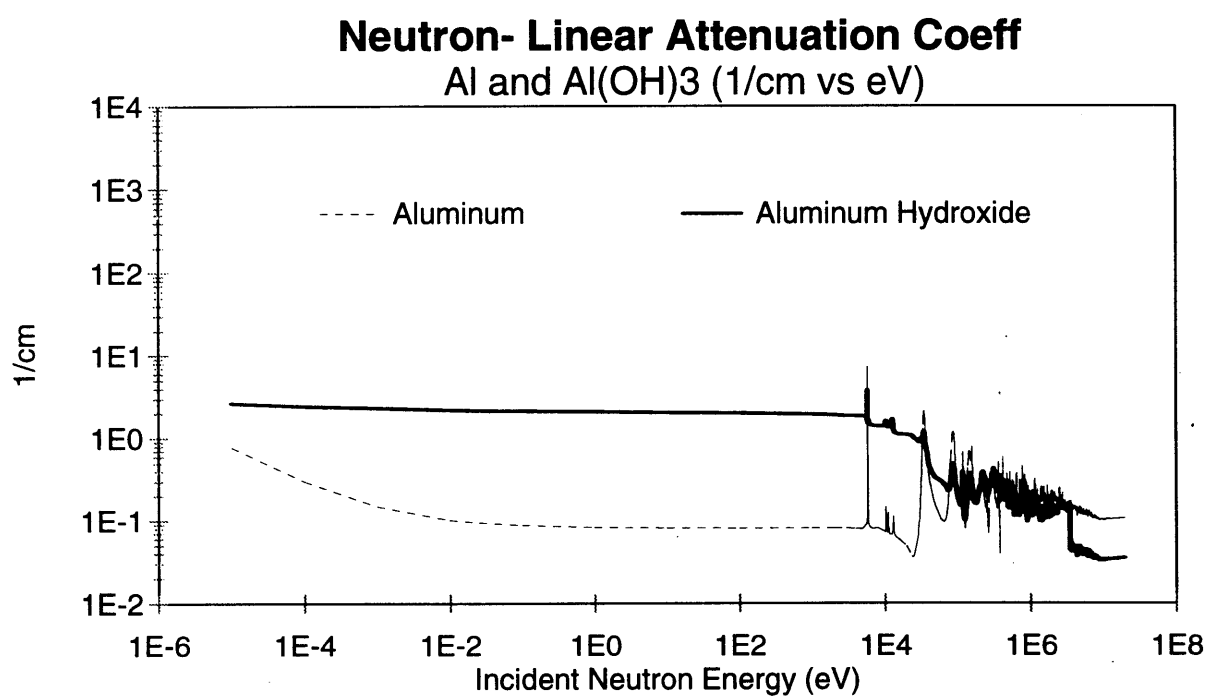

Figure 3.4: Neutron— Linear Attenuation Coefficients for Al and $Al(OH)_3$

3.4. Accelerator Based Neutron Radiography

In general, accelerator based neutron radiography provides a much lower flux source of neutrons than a reactor based systems. Neutrons are produced by inducing a controlled nuclear reaction tailored to neutron production. There are many types of nuclear reactions that could be of interest. A nuclear reaction between a photon and a nucleus can yield neutrons through a (γ,n) reactions. An accelerator can be made to produce gamma rays to initiate this reaction, or a radioactive isotope which decays with the proper energy gamma-ray can be used. Another nuclear reaction which yields neutrons is a radioactive decay of a nuclei. The highest neutron yielding decays are spontaneous fission of material. Finally, there are a number of nuclei to nuclei reactions with which a neutron can be emitted.

^{210}Po-Be	^{9}Be$(\alpha,n)^{12}$C	138 d
^{210}Po-B	^{11}B$(\alpha,n)^{14}$N	138 d
^{239}Pu-Be	^{9}Be$(\alpha,n)^{12}$C	24440 y
^{124}Sb-Be	^{9}Be$(\gamma,n)^{8}$Be	60.9 d
^{252}Cf	Fission	2.65 y

Figure 3.5: Common Radio-isotope Neutron Sources and $t_{1/2}$

Nuclear reactions between two particles can only occur at very close distances, much closer than distances where normal chemical reactions occur. For particle collision reactions, a large amount of energy is needed to bring two positively charged nucleus be in close proximity, because the columbic repulsion must be overcome. This is usually accomplished by giving one or both of the particles a large kinetic energy. One technique is to heat the particles to extremely high temperatures. Another is to accelerate one of the particles with enough energy onto the second particle. This technique is known as an accelerator neutron source, and many variations of it have been created.

^{7}Li(p,n)^{7}Be
^{9}Be(p,n)^{9}B
^{9}Be(d,n)^{10}B
^{2}H(d,n)^{3}He
^{3}H(d,n)^{4}He
^{2}H(t,n)^{4}He

Figure 3.6: Common Accelerator Reactions

The primary concern with non-reactor based neutron sources is that it is difficult to create an intense enough source of neutrons to achieve a strong enough signal to be used for imaging. Of the above mentioned techniques, the accelerator-based neutron source is the only one which has currently been developed far enough to make it feasible for neutron production. Even though this field is very highly developed, the neutron yield is still many orders of magnitude below what is capable from reactor-based sources. Thus, while reactor-based neutron radiography can be thought of as taking photographs in normal lighting conditions, accelerator-based neutron radiography can be thought of as taking photographs by candle light.

Source	Energy Spectrum	Intensity
Reactor	$\leq$ 2 MeV	$\leq 10^{18}$ cm^2/s
Ng Generators	$\leq$ 14 MeV	$\leq 10^{10}$ cm^2/s
^{239}Pu-Be Source	$\leq$ 6 MeV	10^5 - 10^8 1/s
^{252}Cf	$\leq$ 2 MeV	10^8 1/(s-mg)
Linear Acc	Varied	$\leq 10^{14}$ (1/s)
*Our Current System	$\leq$ 2.5 MeV	$\leq 10^8$ (1/s)

Figure 3.7: Characteristics of Neutron Sources

3.4.1. Accelerator Types

Portability and beam strength are our major concerns with selecting the type of accelerator to be used to solve our problem. There are a number of types of accelerators to choose from which fit this requirement. The type our project used was a radio-frequency quadrupole ion accelerator.

3.4.1.1. Direct Current Accelerators

One way to accelerate charged particles is to subject them to large, stationary electric fields. A positively charged ion, for example will be repulsed by a large negative field and attracted by a large positive field. A simple example would be to simply maintain a target material at a very low negative energy, and allow the positively charged ions to be attracted towards it.

The major limitation of such accelerators is that very large electric fields must be generated to create high energy beams. These large fields are difficult to work with, and must be well insulted to prevent unwanted electric discharge. One way to avoid this predicament is to use many small increments in the electric field, in place of one large one. That way, the electric field gradient can be spaced over a much longer distance, simplifying the insulating requirement. DC machines are an attractive option because of their relative simplicity both in design and maintenance.

It is possible to use a DC machine as a portable neutron source. However, in many cases they are prohibitively large to be feasible as a portable neutron source. Their size is limited by field gradients of $\leq$ 1 MeV/m. In addition, they are limited by the amount of amount of current they can put on target, and thus the neutron flux they can produce.

3.4.1.2. Radio Frequency (RF) Accelerators

The limitation of working with large static electric fields can be overcome using electromagnetic fields. Many different types of devices have been built using radio-frequency waves.

The most basic of these is a linear radio frequency (RF) accelerator. Essentially, an oscillatory wave is introduced into a chamber containing charged particles. Particles are "pushed" one way during an increasing electromagnetic wave. They are then shielded from the decreasing electromagnetic wave, which would otherwise have the effect of "pulling" them back, and decelerating them. The net effect is to continue to push them in one direction. Like DC machines, the particles can be accelerated to higher energies by multiple steps, rather than introducing a large enough field gradient to accelerate them at once. As the particles gain speed, they can be introduced to a more rapidly changing electromagnetic field by either increasing the frequency of the radio-wave or by increasing the amplitude of the radio-wave.

Rather than introducing the particle to a series of waves, it is possible to accelerate the particle by having it travel with a single propagating wave, essentially "riding the wave". As the

propagating wave increases in frequency, the increasing field gradient that the acts on the particle will accelerate it in perfect sync with the propagating wave peak.

Because the acceleration caused by electric field gradients in RF accelerators are controlled by both frequency and amplitude (magnitude of the field gradient between the minimum field and maximum field) of the RF wave-- and not, as in DC accelerators, solely by the magnitude of the field gradient between minimum and maximum static fields-- large gradients can be created without using very large amplitudes in the RF field.

If the length of the accelerator is not a major concern, very low frequency radio waves, with very long wavelengths can be used. In general, these designs have been limited to around 10 MeV/m. The accelerator can continue to modulate the frequency or the amplitude in multiple steps to achieve extremely high accelerations. An example of this is the LINAC found in Los Alamos, which extends for over a half mile, and creates a beam energy in excess of 800 MeV, or 85% the speed of light.[1] The Stanford Linear Accelerator (SLAC) is two miles long (3.3 km) and creates a beam energy of approximately 33 GeV.

The RF power required for a linac is governed by the equation:

$$P \approx \frac{C\,E^2\sqrt{\lambda}}{L} \tag{3.4}$$

<u>where</u>: E = *Desired Particle Energy (eV)*
$C \approx 10^{-7}$ *for protons*
L = *Acceleration Length (m)*
λ = *RF wavelength (m)*

It is evident from this equation that much more power is required for compact, shorter length accelerators.[2]

The beam must be focused to prevent the beam from spreading out and hitting the walls of the accelerator. One easy method to accomplish this is to again use electric fields.

Another method of focusing and accelerating the beam is to use a series of symmetrical RF waves. Our system uses quadrupole configuration, which instead of creating a single radio wave, four waves are created at the four corners of a box-like geometry. The waves that oppose each other across the diagonal of the box are in phase with each other, and 180° out of phase with the two adjacent waves. This geometry focuses the beam sharply into the center of the chamber. It also accelerates particles whose initial velocity exactly matches the initial velocity of

---

[1]LAMPF Introductory Booklet LA-UR-87-327. Jan 1987. pp. 1-38.

[2]Livingston and Blewett, 322.

the propagation of the field in the transverse plane at the entrance to the chamber. Again, with this configuration, the accelerating gradient is produced by increasing the frequency of the wave as it propagates in the transverse direction. A radio frequency quadropole has the added advantage of being very compact. This meets our requirement of portability.

If very high energy beams are required, and length of the accelerator is an issue, as it would be for a portable, less expensive machine, there are other methods that may be used. One of them is found in a RF cyclotron. A cyclotron introduces a magnetic field into the chamber which causes the particles to follow a circular orbit. Again, they are introduced to a positive field gradient caused by part of an electromagnetic (usually radio-frequency) wave. As the particle increases its speed, its orbit around the center of the magnetic field increases. Thus, as the particle accelerates, it follows a circular orbit, which spirals out with a greater orbiting radius. Particles are extracted from the outside radius.

While Cyclotrons are much more compact than linear RF accelerators, their size bears a strong relationship to the strength of the magnetic field. The strength and uniformity of the magnetic field inhibits them from being used as a portable neutron source, yet makes them attractive as a stationary accelerated ion source. However, for a low energy beam, a Cyclotron could potentially be made into a portable neutron source.

3.4.2. Accelerator Ion and Target Selection

There are many types of targets to choose from, and target selection must be done from a number of different criteria. First, it is important that the proper ion and target material be selected to give as many neutrons as is possible. Second, the target material must be able to dissipate the heat of the reaction without failing. Third, the target must be capable of dissipating the electrical charge that will build up as positively charged ions impinge upon it. Fourth, the target must not interfere with the high vacuum environment of the accelerator.

There are a large number of neutron producing reactions, and therefore a large number of possible ions and targets that we could select. As it takes less energy to accelerate lighter ions, it is preferable that a hydrogen isotope be used, the lightest positively charged ion. Hydrogen is an excellent first choice, for there are a number of proton reactions that produce neutrons. In addition, hydrogen is easily available.

The deuteron ion, however may have a few advantages over hydrogen. Although it is heavier, and considerably more expensive than hydrogen, the deuteron reactions are more prolific in the number of neutrons they produce. Tritium might even be better, although it is prohibitively expensive and there are a number of issues related to the fact that it is radioactive.

For target materials, a major constraint is that it should be a stable solid at high heats and high vacuum. One of the best suited materials, that also is prolific in its neutron production is ^{9}Be. Although beryllium is highly poisonous, it is stable and can be brazed onto a metal surface. Thus, it can dissipate its heat directly to the metal. Heat deposition is a very serious design problem for high energy, high current beams. Many elaborate solutions have been devised to try to solve it. For example, the LAMPF accelerator at Los Alamos uses a spinning target to keep

the beam from locally heating the material and vaporizing it.[3]

A gas target would have to be maintained at a pressure significantly higher than the pressure (10^{-5} Torr or lower) required in a typical accelerator chamber. One way of accomplishing this would be to have a window between the accelerator chamber and the gas target. Unfortunately, even a very thin window (10 μm) would attenuate the charged particle beam significantly, and this attenuation would deposit enough heat on the widow to vaporize any material, unless it were significantly thicker than 10 μm. Of course, a thicker window would attenuate all the beam, and the goal of a gas target would be defeated.

Iverson at MIT has recently developed a windowless gas target[4]. The target works by focusing the beam to a very small diameter. The higher pressure gas target chamber is separated from a second chamber by a valve which consists of a small aperture a little larger than the beam diameter. The second chamber is held at a lower than the gas target with a turbo vacuum pump. The small aperture between the chambers minimizes the amount of gas lost from the gas target to the lower pressure chamber. The pump which evacuates the intermediate chamber recirculates the deuterium into the high pressure target chamber. There are two of these pressure "step-down" chambers in series before the vacuum chamber of the accelerator. To further increase the efficiency of the valves between the first and second chamber and the target and the first chamber, the valve is closed in between accelerator pulses. To accomplish this, a disk with a small slot cut in it rotates in sync with the pulsed beam to seals the aperture between the high pressure gas target and the low pressure chamber when the accelerator is between pulses.

The gas target serves four main purposes. The first is that it allows us to take advantage of a number of neutron producing reactions with gasses that were previously not possible. Many of these reactions have the potential to increase the neutron yield significantly. The second is that the composition of the target can actually be changed during operation (without elaborate switching magnets), allowing gasses at different pressures to be used. The gas target is a "thin" target, creating a neutron spectrum with a relatively low spread in neutron energies. Finally, the gas target can allow significantly more energetic beams to be used without the thermal cooling requirements of most solid targets. The hot gas can be cooled away from the neutron reaction by drawing off the hot gas, cooling it, and then returning it to the target.

3.4.3. General Moderator/Collimator Design

A moderator is used to slow the incident neutrons to thermal energies as well as to provide a partially collimated beam of neutrons for our imaging system. The neutron spectrum from both the $^{9}Be(d,n)^{10}B$ and $^{2}H(d,n)^{3}He$ contains primarily fast neutrons up to 4.7 MeV. We must create a collimated beam of thermal neutrons for our imaging purposes.

The moderator's first job is to reduce the energy of a maximum number of these neutrons to a useful thermal energy. It does this primarily through collisions in a region known as the

---

[3] LAMPF Introductory Booklet LA-UR-87-327. Jan 1987. pp. 1-38.

[4] Iverson, Erik, "A Windowless Gas Target"

"moderator". One of the most common ways to reduce the energy of the neutrons is through elastic collisions with very light particles. Light particles are ideal for elastic collisions, because the allow much higher energy transfers per collision than heavy particles. The equation that governs these collisions will be discussed more completely in section 6.8:

$$E_{max} = E_o (1 - \alpha)$$

$$\underline{where}\ \alpha = \frac{A - 1}{A + 1} \tag{3.5}$$

A = atomic weight of target nucleus (amu)
E_o = Initial energy of neutron (MeV)
E_{max} = Maximum energy transferred to target nucleus (MeV)

Because neutrons will have to undergo multiple collisions before they moderate, the moderator must have a much higher probability for scattering neutrons than absorbing them ($\sigma_{Scattering} >> \sigma_{Absorption}$). It is important to keep the neutrons concentrated in one region if we expect to have a concentrated beam at our scintillator, so it is important that our moderator have as many atoms per square cm as is possible (high density for a given atom).

Hydrogen (^1H) is a well suited for moderator material. As the lightest element, it would absorb the most energy by elastic interactions in the fewest collisions. Furthermore, the cross-section for scattering is much larger than that for absorption. Two relatively high density hydrogenous materials are commercially available for use: water and poly-ethylene. Deuterium is a heavier material, requiring more collisions to slow down the neutron, however, its absorption cross-section is even lower than that of water. Again, heavy water and plastic materials with high deuterium concentration are readily available, though much more expensive the ^1H. Other materials, such as graphite, have been used successfully as moderators based on the same criteria.

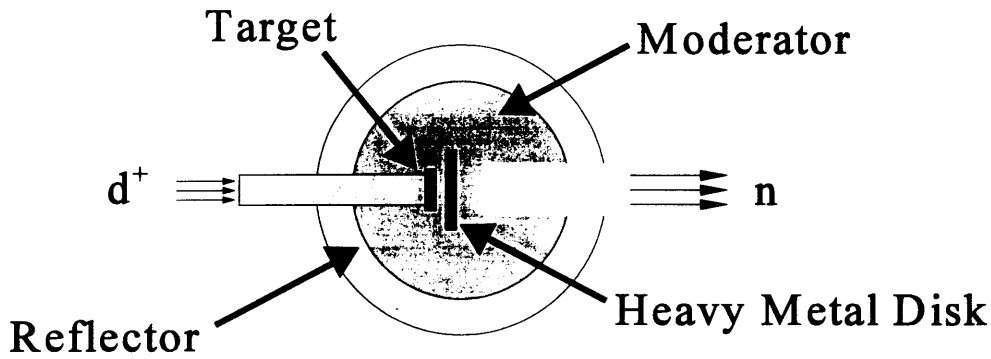

Figure 3.8: Moderator Design

Fast neutrons often have a very low cross-section for interaction with the moderator material. To prevent them from escaping the cavity completely, a reflector is generally used to knock these materials back into the moderator. The reflector material usually encases the moderator material. With a reflector, as with a moderator, collisions should be much more probable than absorption reactions, and the density of the material should be very high to keep the neutrons concentrated to a small area. Unlike the moderator material, however, it is more important that the reflector change the direction of the neutron than absorb its energy. So ideal reflector materials are usually very heavy nuclei, such as lead. However, increasing the likelihood of collisions interactions ($\sigma_{Collisions}$), decreasing the likelihood of absorption interactions ($\sigma_{Abosrption}$), and concentrating the atoms may all be more important than the density. This explains why much lighter nuclei, such as carbon, have been used very successfully.

Another way to keep the neutrons concentrated in the moderator is to slow them down immediately after production, decreasing the distance they will travel in the moderator before interaction with it. One way to do this is to have the neutrons undergo inelastic collisions (n, nγ) or knock out collisions (n,2n) immediately after they are produced by placing a thin stip of heavy metal a short distance from the target, before the moderator. Fast neutrons often have a very high probability of such reactions with materials such as tungsten (W), copper (Cu), and lead (Pb). These materials do not thermalize neutrons, so they are most effectively used in conjunction with actual moderator material. An example of this was the work of Cluzeau and Tourneur.[5] This material is much less important for lower energy neutron spectrums.

If the moderator (moderator/reflector/heavy metal) is designed well, there will be an area where the thermal neutron flux peaks known as the Thermal Neutron Peak (TMP). One of the goals of proper moderator design is to maximize the TMP flux. If the TMP point is known, a hole can be made in the moderator to allow the thermal neutrons to be drawn off. The ratio of the length of the hole (L) to the diameter of the hole (D) controls the collimation of the beam (L/D). A well collimated beam does not allow neutrons to escape unless they are all going in the same general direction. This is extremely important in imaging. The sharpness (ie: spatial

[5]Cluzeau, S. and P. Le Tourneur, Upgrade of the Diane Performance", pp 1-3.

resolution) of the "shadow" a phantom casts depends on the collimation of the beam and the size of the source.

Designing an actual moderator is an extremely complicated process because there is a large coupling between the geometries of the moderator, reflector, heavy metal, and moderator hole. This will be discussed in greater detail in chapter 10. Moderator design is commonly done using computer generated Monte Carlo simulations.

4. Nuclear Imaging Techniques: Radiation Detection

The detection device must actually serve multiple purposes. First, it must obviously detect the radiation. Second, it must store the detected radiation over the entire exposure in a reliable manner, maintaining desired spatial resolution. It must be sensitive to the differences in radiation which are created by selective attenuation in the phantom. Finally, it must record these differences over the entire exposure time and provide a reproduction of the results. These criteria are shown in Figure 4.1.

Radiation Detector Criteria:

- ♦ Detect radiation used by imaging technique
- ♦ Collect and store detected radiation over entire exposure
- ♦ Must meet spatial resolution requirements
- ♦ Be sensitive enough to changes in radiation to detect differences in attenuation
- ♦ Provide reliable reproductions of the results
- ♦ Should have linear response if possible

Figure 4.1: Criteria for Radiation Detection

4.1. Direct Exposure of a Radiation Sensitive Film

Film can meet most of the criteria with the exception of linear response. Films are made which are sensitive to many types of radiation. The most common example is light sensitive film used in the everyday camera; however, films exist for both x-ray and neutron detection. Interaction with the radiation changes the film chemically during the entire exposure time. Film maintains spatial resolution. The sensitivity can be controlled by the type of chemicals used. Then, the film can be developed, and the negative it produces provides a reliable means of reproducing the results.

Films have many advantages. They are relatively inexpensive, and are a well developed technology. They are simple to use, and are made for a number of different uses. A film based detection system can achieve very high spatial resolution, which varies depending on the sensitivity of the film and the type of radiation used. multiple levels of sensitivity are possible through the combination of different chemical composition and exposure times.

However, film has many disadvantages. While it can achieve many different levels of sensitivity, it does not exhibit a linear response to radiation. Thus, it is really only optimized for a particular sensitivity, and it will be relatively insensitive to others. This has the advantage of showing excellent contrast for the sensitivity region in question, but poor response for other areas. Because the sensitivity is frozen based on the film type and the exposure length, it is difficult to post process the film to look at areas of different sensitivity. There is little flexibility in sensitivity-- the sensitivity must be known before the exposure and the purchase of the film, and to look at areas of different sensitivities, it would be necessary to take separate images.

Another potential disadvantage of direct radiation sensitive film techniques are limited to the spatial resolution of the film. While the spatial resolution of light-sensitive films can be extremely high, the spatial resolution of x-ray and neutron-sensitive films are much lower. In addition, very large films (necessary for very large images) can be very expensive.

Finally, film suffers from efficiency and noise collection. While light-sensitive film may capture a high percentage of the incident photons, x-ray and neutron films have much lower efficiencies. This means that for x-rays and neutrons, the information from a large percentage of the radiation is lost. Noise is added to the system through unwanted response to other types of radiation, or through non-linear response to the imaging radiation source. Films can be quite sensitive to other forms of radiation such as x-rays and light.

4.2. Coupled Scintillator- Film

For radiations other than light, it is possible to convert the radiation into a light signal using a scintillator screen. Scintillator screens capture the energy of the radiation and retransmit it as visible light. This separates the first criteria of Figure 4.1 from the others making it possible to optimize it independently. The radiation would strike a scintillator screen, giving off light which is focused via a lens onto a light sensitive film.

This has a number of advantages over a direct exposure of a radiation sensitive film. In some configurations, the scintillator screen can be made to have a much higher efficiency than films, allowing better use of the radiation. In addition, in some cases, scintillator screens can be made less sensitive to other radiation sources, preventing false signals and background noise. Light sensitive films are used to store the information, eliminating the more expensive x-ray and neutron sensitive films. In addition, there are a wider selection of commercially available light-sensitive films and cameras.

Another potential advantage is that the detection system can be optically coupled to the recording system allowing more flexibility in resolution tradeoffs. Mirrors and lenses can be used to move the film out of the path of direct radiation to which it may be sensitive. This helps remove unwanted background noise. The optical coupling allows for light intensifies or filters to be used to increase the gain or remove noise from the system. The optical coupling also allows more flexibility in designing the limiting resolution of the system by allowing the photographer to select a minification (ratio between the height of the object photographed and the height of the image projected on the screen) desired.

Tradeoffs of Optical Coupling:

Advantages	Disadvantages
♦ Independent control of minification	♦ Loss of Light
♦ Separation from unwanted radiation source	♦ Added Complexity
♦ Ability to optically condition signal (intensifiers, filters)	

Figure 4.2: Tradeoffs of Optical Coupling

Coupled Scintillator-Film systems, however, have drawbacks. In addition to suffering from many of the disadvantages of a direct exposure of a radiation sensitive film, such as non-linear film response, this system has a few new problems. The scintillator screen (and light intensifier, if used) will add noise to the system, characterized by its gain and spread of light. It

some cases the scintillator screen will have a worse resolution than the direct exposure radiation film. In addition, the sensitivity of the system may be degradation depending on the gain of the scintillator (light output per radiation event) and the quality of the optical system, which can only capture a portion of the light. This sensitivity will also put limits on the minification of the system.

4.3. Optically Coupled Scintillator- CCD Detector

Another configuration uses a scintillator screen optically coupled to a CCD detector. A CCD detector (Charge Coupled Device) is a micro-electronics chip containing an array of photo-diodes sensitive to visible light. The CCD serves four main functions. First, it converts photons to electrons maintaining a certain level of spatial resolution. Second it collects the electrons in capacitor wells, known as pixels. It then coverts the number of electrons it has collected into a voltage signal. Finally the image can be digitized and put onto a computer. The chip consists of an array of capacitor wells, the size of which define its spatial resolution.

Since the detector is separated from the collection device, the system gains the advantages being able to optimize the detect independent of the collection device. The system also gains both the advantages and disadvantages of an optically coupled device.

There are many advantages to using a CCD Detector in place of film. Its primary advantages over film are its linear response to light and low noise. Many CCD detectors are available with varying well sizes and array sizes.

However, these advantages come at a price. CCDs have much lower spatial resolution than films and are limited in size to a few inches. Low noise CCDs are extremely expensive compared to film prices. Large CCD's are limited in the speed in which they can take pictures, and quickly impose memory constraints in image storage. Finally, CCDs can add a level of complexity in that they require computers to handle and process the information. It should be noted that all of these factors are drastically changing as the technology of CCDs improves, even the last constraint about complexity, as computers become more common and accessible.

CCD chips come with many different capabilities. The physical size of each pixel will factor into the total system resolution. It is common to find modern CCD chips with square pixels between 10 - 15 microns on an edge. However, it is possible to purchase CCD chips with larger or smaller pixel arrays. For example, our pixel arrays are 22.5 microns on each edge. For a non-optically coupled system, the size of a pixel may directly control the spatial resolution of the system, as will be discussed later.

Another important characteristic is the total number of pixels, or array size, of a CCD chip. Array sizes can be quite large. For instance, CCD chips are available as large as 4000 x 6000 arrays (Dalsa Corp). Larger pixel arrays present many challenges to the overall system design due to the large amount of information that must be dealt with (16 million pixels!). However, for an optically coupled system, the combination of the pixel size and the array size may control the spatial resolution of the system for a given image size. This will be discussed in greater detail in subsequent chapters.

The CCD's characteristics are also measured by its dynamic range, the accuracy with which it can determine the number of electrons in a given pixel. This is largely dependent on

both the signal to noise ratio of the pixel and the Analog to Digital (A/D) conversion accuracy and resolution. Typical low cost A/Ds for CCDs produce an 8 bit digital signal corresponding to the number of electrons in each pixel. It is possible to buy more expensive CCDs with higher dynamic ranges of 16 or 20 bits. The maximum pixel capacitor well size is less than 10^6 electrons, so the maximum required dynamic range is 20 bits. However, to fully utilize a higher dynamic range, the noise must be less then the accuracy of the last significant digit. As will be discussed in greater detail, the A/D roundoff error of the last significant digit adds a noise to the overall system noise.

A final measure of CCD performance which is vital to our experiment is the CCD readout rate. In earlier designs of CCDs, every pixel went through the same A/D to be digitized. As the arrays got larger and larger, the readout time of the A/D became more critical. For example, a CCD with 1 million pixels would take 10 s to readout at a 100 kHz A/D rate. An obvious way to read out a CCD faster than the A/D conversion rates was to use multiple A/Ds in parallel. As a result, very large cameras (> 1,000 x 1,000 pixels) have been designed with fast frame rates (> 30 Hz), by using parallel systems.

4.4. Spatial Resolution

The spatial resolution of the system will be controlled either by the spatial resolution of the beam, the radiation detection device (film or scintillator device), the secondary radiation collection device (film or CCD), or the way these last two elements are optically coupled. As discussed in section 3.4.3, the spatial resolution of the beam will be controlled by how well the beam is collimated as well as the amount of small angle scattering that occurs. The spatial resolution of the detection device is controlled by area of secondary radiation that results from a detected event. The spatial resolution of the secondary radiation is controlled by detector size. Optical coupling which either minifies or magnifies the signal from the radiation detection device before it is detected by the secondary radiation collection device will also have the effect of minimizing or magnifying the spatial resolution of the secondary radiation detection device.

For example, assume our system used a relatively well collimated neutron beam to conduct neutron radiography. We used a neutron scintillator screen that produces a light peak per detected neutron event that has a 100 μm half width maximum, which, for the purpose of this example, we will model as a circle with a diameter approximately equal to 100 μm. If we CCD with a square pixel size of 22.5 μm x 22.5 μm, without optical coupling, the spatial resolution of our system would be limited by the 100 μm resolution of the scintillator screen. However, if we manipulated the signal from the scintillator screen optically, and focused it into the CCD as an image 1/10 its original size, we would then have a system resolution which was limited by the pixel size. Overall, the system resolution would limited by the magnified dimensions of our pixel, μm x 22.5 μm. The system resolution can be evaluated with an edge response test.[6]

The spatial resolution of a film can be significantly better than that of a CCD camera,

---

[6]Shi, Shuanghe, "An Accelerator-Based Neutron Imaging System and Its Application to the Detection of Corrosion in Aircraft", pp 114-121.

especially for large images. The non-linear response of the film, coupled with the complications of chemical processing, however, strongly offset the gains in resolution.

Section 2: Experimental Design of a Quantum Limited Detector

5. Experimental Setup

5.1. Neutron Production

For a neutron source, we use a DL-1, RFQ Neutron Generator developed by AccSys Technology Inc. Our accelerator produces a pulsed beam of 900 keV deuterons onto a Beryllium Target. Neutrons are produced by either the $^{9}Be(d,n)^{10}B$ reaction or the $^{2}H(d,n)^{3}He$ Reaction. The following sections outline the characteristics of our neutron production.

5.1.1. Deuteron Ion Production and Acceleration

Our system produces deuteron ions by ionizing deuterium gas in a duoplasmatron ion source. A filament is ohmic heated by passing a large current through it. This boils off elections, and partially ionizes the surrounding gas. An arc is then struck across the partially ionized gas in pulses, ionizing it considerably further, and producing 80-90% d^{+}, with the remaining ions being d_2^{+}. An electrostatic field of 25 kV is used to extract the ionized particles into the acceleration chamber. Deuterons are focused and accelerated by a quadrapole radio-frequency accelerator. 425 MHZ RF drives the quadrapole, which accelerates d^{+} ions to a mono-energetic beam at 900 keV. The beam delivers up to 10 mA during a pulse and can have a maximum pulse width of up to 100 μsec, but there is a 5 μsec fill time. It has a maximum repetition rate of 640 Hz. The accelerator weighs 450 lbs and is only 4 ft long, making it small enough to be a portable source. Our RF power supply is limited to a duty cycle not to exceed 2.25%. It delivers approximately 60 kW peak at 425 MHZ.

5.1.2. Accelerator Beam Targets

We have four operational targets. The first three are solid Be targets of various geometries. At 900 keV, our Be targets produce approximately 7.8×10^{7} neutrons/(μA d+), which can be expressed as a target efficiency of $\eta_{Target} = 1.2 \times 10^{-5}$ n/d+. An intense, point like source of multi-energetic neutrons is produced. At the currents that our accelerator puts on target, heating of the beryllium is not an issue.

The $^{9}Be(d,n)^{10}B$ reaction is exothermic (Q = 4.36 MeV) and prolific in its production of neutrons, as shown by the figure on the following page. The deuteron absorption by ^{9}Be creates an excited, unstable ^{11}B atom, which decays by the emission of a neutron to ^{10}B. The ^{10}B may decay to either the ground state, or to an excitation state of either .72 MeV, 1.74 MeV, 2.15 MeV, or 3.59 MeV. The neutron yield from each state is shown on the following page:[7]

---

[7]Watterson, J.I.W. and R.C. Lanza, "The reaction $^{9}Be(d,n)^{10}B$ as a source for fast and thermal neutron radiography", p 1.

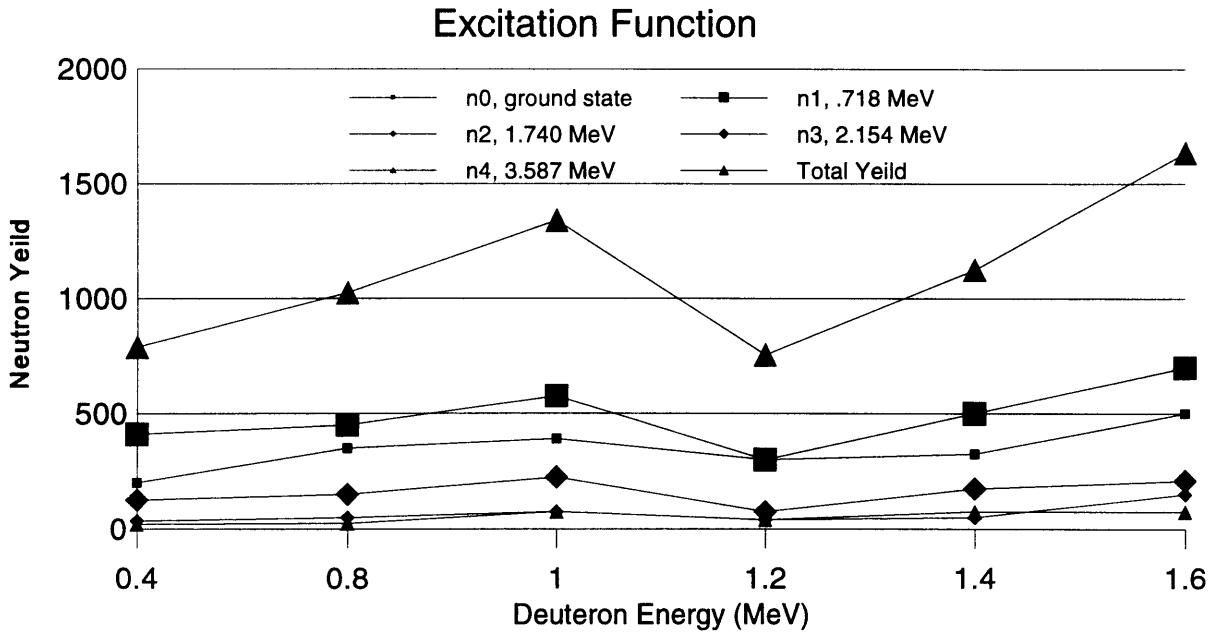

Figure 5.1: Excitation of the $^{9}Be(d,n)^{10}B$ for the Ground and First Four Excited States of ^{10}B (From Shepetnyi)

If ^{10}B is left in a higher excitation state, the energy of the neutron is less. The relative ratios between the states as well as the total yield are very strongly dependent on the incident deuteron energy. An important result of this is that the number and ratio of lower energy neutrons emitted increases significantly from 900 to 1100 keV. This spectrum was measured by Watterson and Lanza and the results are shown below:

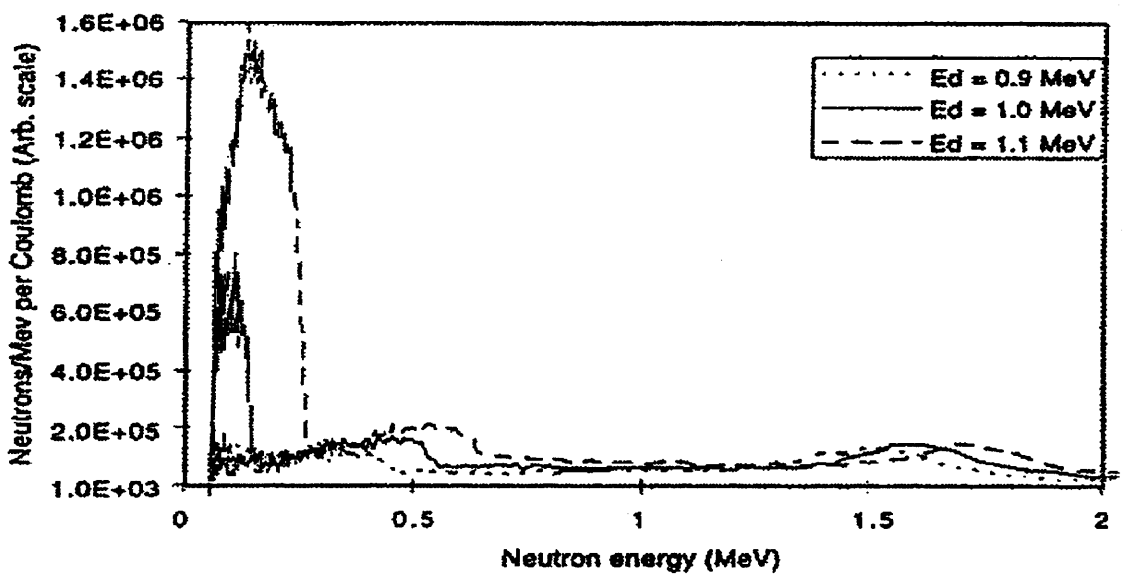

Figure 5.2: Neutron Yield for $^{9}Be(d,n)^{10}B$ at Three Different Incident Deuteron Energies

It is evident that there are significantly more low energy neutrons from the 1.1 incident MeV deuteron beam than from the lower energy deuteron beams. This is due to two different effects. First, we expect a higher total neutron yield at the higher deuteron energy. The second effect is that we also expect a greater low energy neutron yield due to a relatively large number of neutrons that are emitted leaving ^{10}B in a higher energetic state. As will be discussed in greater detail, this will be an important method to improve the thermal neutron yield of our system.

The second type of target is a newly developed windowless gas deuteron target. The gas target, described in section 1.4.2, page 19, maintains deuterium gas at approximately one tenth of an atmosphere (.1 atm), while still maintaining a vacuum in the accelerator chamber. At 900 keV, the gas target will produce significantly more neutrons than our Be targets. In addition, the gas circulated in the target can easily be changed to use another reaction.

5.2. Neutron Moderation/Collimator

General moderator design has been discussed in section 3.4.3. The moderator for our system has changed from experiment to experiment, and is not even close to ideal. Moderator design is a complicated time-consuming process, and was beyond the scope of this project. A new moderator design has been conceptualized, and is currently being modeled on MCNP. Pending the completion of that moderator, between 3-10 1" sheets of polyethylene where used in various geometries in an attempt to experimentally maximize thermal neutron production. One of the contributions of this work has been the postulation of a systematic technique to moderator which will maximize thermal neutron production.

5.3. Neutron Detection for Imaging

Our neutron detection system has attempted to exploit the many advantages of a CCD - Scintillator coupled system. It has been designed and optimized for a neutron radiography technique which uses long exposure lengths (< 300 s).[8] It has 6 main components: neutron scintillation, optical focusing, photon detection by a cooled CCD camera, analog signal processing, analog to digital conversion, digital signal processing.

5.3.1. Neutron Scintillator: Neutron to Photon Conversion

Our system used two different Li^6-ZnS thermal neutron scintillator screens. Both were manufactured by Levy-Hill. The scintillator produces a large number of photons per detected neutron. The neutron is captured by Li^6, which has a large thermal cross-section for neutrons (945 barns). A tritium and helium ion are produced by the following reaction:

---

[8]Lanza, R.C, S. Shi, and E.W. McFarland, "A Cooled CCD Based Neutron Imaging System for Low Fluence Neutron Sources."

$$Li_3^6 + n_0^1 \rightarrow He_2^4(2.05\ MeV) + H_1^3(2.73\ MeV) \quad (5.1)$$

The tritium ion (H^3) and the helium ion (He^4) are quickly stopped by the ZnS phosphor, and the energy is released as 400 nm photons. The phosphor has a relaxation time of 2.5 μs.

There is a tradeoff between the ratio of the Li^6 detector and the Zn-S phosphor. Increased Li^6 content in the screen will improve the detection efficiency at the expense of replacing some of the Zn-S scintillation material, which increases the number of photons given off per neutron event.[9] For example, the Nuclear Enterprise (NE) -426 is 180 x 240(mm) and has a detection efficiency of 15%. The Levy-Hill Scintillator has a detection efficiency of 45%, and as a result, the gain is expected to be significantly lower than that of the NE 426.

This screen has been tailored for our use by adding a Cu activator in place of standard Ag activator, which will shift the light emission spectrum of the phosphor towards the green. This was done to because our CCD has a better detection efficiency and gain for green light compared to that of blue.

It is interesting to note that our current system can easily be made to do either fast neutron or x-ray radiography. These experiments were done by replacing our scintillator screen which has been optimized for thermal neutrons with either a fast neutron, plastic scintillator screen, or a gadolinium gamma ray scintillator screen. This makes switching from detection one form of radiation to detecting another quite trivial from an equipment standpoint.

5.3.2. Optical System

A lens was used to couple the scintillator screen to the CCD detector as follows:

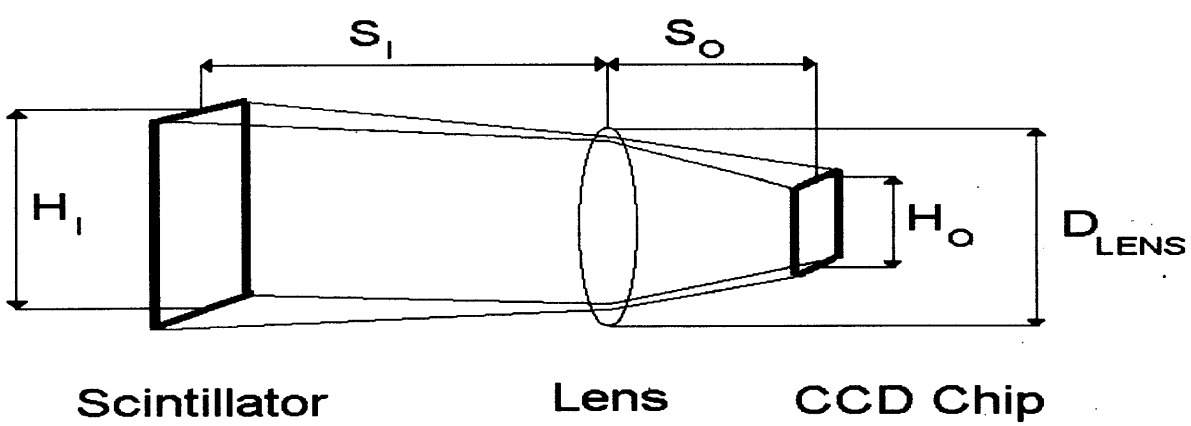

Figure 5.3: Diagram of Lens Coupled System

[9]Spowart, "Optimising Neutron Scintillators for Neutron Radiography"

The distance from the scintillator and the lens is known as the object distance (S_O). The distance from the lens to the CCD Chip is know as the image distance (S_i). The minification is defined as the ratio between the object height and the image height:

$$m = \frac{H_O}{H_i} = \frac{S_O}{S_i} \tag{5.1}$$

The object distance and the image distance are related to each other by::

$$\frac{1}{S_O} + \frac{1}{S_i} = \frac{1}{f} \tag{5.2}$$

<u>*where*</u>: f = *focal length of lens*

Combining these two equations gives us the relationship between the minification, the object distance and the focal length:

$$S_O = f\,(1 + m) \tag{5.3}$$

From this equation, it becomes evident that varying the object distance has the result of changing the minification of the system. Another useful measure of the sensitivity of the lens is the F number defined as:

$$F = \frac{f}{D_{Lens}} \tag{5.3}$$

We had two different lenses at our disposal. The first is a F=.95, f = 100 mm lens (Perkin Elmer), and the second is a F=1.2, f=50 mm lens (Nikon).

5.3.3. Photon Detector: CCD Camera System

Our system used an EEV 1242 x 1152 CCD Chip. The active detector area of the chip is 2.56 cm x 2.59 cm, with 22.5 μm x 22.5 μm pixels. Our chip is cooled using a thermoelectric (Peltier effect) cooler. Heat is then removed from the thermoelectric device by convection to a circulating cooling fluid of either air or water. Our chip can be cooled to -40° C by blowing air

over the thermoelectric device, or to -50° C by circulating water over the cooling device. Lower temperatures can be achieved by using a refrigerant system or by using cryogenic cooling to cool the thermoelectric device.

Our CCD chip is supported by a Princeton Instruments ST-138 Controller box, which does analog double correlated sampling before the A/D conversion. This will be discussed in greater detail in Chapter 6. The ST-138 has the ability to do two analog to digital (A/D) conversion speeds. The first is a 1 MHZ, 12 bit A/D, and the second is a more sensitive 430 kHz, 16 bit A/D.

5.3.4. Digital Signal Processing: P6-200MHz PC

The box interfaces with a Macintosh Quadra 650 via a Princeton Instrument's proprietary fast serial link. Our system acquires the image using IPLab software (Spectrum Analysis) package. Data is transferred via Apple Talk to a Pentium-Pro, 200 MHZ computer. Our system did much of the signal processing digitally, using IDL image processing software (Research Systems, Inc).

6. Signal Calculations and the Propagation of Noise

Each analog component in the system must be optimized to maximize the ratio between Neutron Signal to System Noise (S/N) given the constraints of our system.. The overall noise of our system is the combined noise of each of the components. Each of the noises is normally distributed, and independent of each other. Therefore, each component's noise can be combined in quadriture to determine the total system noise.

A large number of techniques have been developed to remove noise from neutron radiography systems. The most straight-forward techniques involve reducing individual components noise, while the more complicated techniques involve high-speed gating and noise filters. Note that the optimum system would have a noise limited only by the statistical noise of the neutrons, know as a quantum limited system. The goal of this design study is to approach this system.

Our signal begins as a flux of multi-energetic neutrons from our neutron generator, and ends as an image created from our detector array. This chapter will trace the signal from beginning to end, showing how the desired signal can be detected and how noise propagates through our system.

6.1. Neutron Production

Our signal starts as a current beam of deuteron ions, I_{D+}, that impinge upon a ^{9}Be target to produce neutrons. Most of the incoming deuterons will not get close enough to the ^{9}Be due to columbic scattering. A small percentage, however, will undergo the exothermic reaction $^{9}Be(d,n)^{10}B$. As mentioned in the section 5.1, the spectrum of neutrons that come off is multi-energetic. Because most have much more energy that neutrons at room temperature, they are known as fast neutrons. The efficiency of the target in producing neutrons, $\varphi_{\text{Fast Neutrons}}$ can be represented by an efficiency, $_{\eta\text{Target}}$. Thus:

$$Neutron\ Flux = \varphi_{Fast\ Neutrons}\ (t) = \eta_{Target}\ (I_{D+})\ (t) \tag{6.1}$$

Neutrons are produced at our target, along with a large amount of unwanted radiation, such a gamma and x-rays. Our neutrons are multi-energetic, extending to 4.7 MeV. Our imaging system depends on attenuation differences between materials, for thermal neutrons. This gives us two problems: how to maximize the number of collimated thermal neutrons produced for our signal, and how to eliminate the signal obtained from unwanted radiation, such as fast neutrons or gamma-rays.

A moderator is used to create and direct a beam of collimated thermal neutrons φ_N, from the Multi-Energetic Neutron Beam produced at the target, onto our phantom. Ideally, every neutron produced would be slowed down and collimated, but practically, only a percentage of them are. This is represented by efficiency, $_{\eta\text{Mod}}$:

$$\textit{Thermal, Collimated Neutron Flux at the Phantom} = \varphi_N\ (t)$$
$$= \eta_{Mod}\ \varphi_{Fast\ Neutrons}\ (t) = \eta_{Target}\ \eta_{Mod}\ (I_{D+})\ (t) \tag{6.2}$$

The collimated neutrons are directed toward the phantom to be imaged. The phantom will attenuate a percentage of the material, the amount of which will depend on the type of material in the target. The attenuation of the neutrons is represented by an attenuation coefficient for thermal neutrons, μ_N, and the thickness, x, of the material. The neutron signal, S_N, after passing through the target can be represented by:

$$S_N = \varphi_N\ e^{-(\mu_N)\ x}\ (t) = \eta_{Target}\ \eta_{Mod}\ I_D\ e^{-(\mu_N)\ x}\ (t) \tag{6.3}$$

The neutron beam is a series of random, independent events, and therefore are governed by Poisson statistics. A detector will detect a fraction of the incident neutrons, known as its detection efficiency (η_{Scint}). For example, a series of experiments with an individual detectors, under identical exposure conditions to a neutron source will yield the same value for the mean value of detected neutrons ($S_{Detected}$) and the variance from the mean. Therefore, the neutron signal of the detected signal has a noise ($\sigma_{Detected}$, represented by a single standard deviation) given by:

$$\textit{Total Neutron Signal} = \textit{Detected Neutron Signal} \pm \textit{Detected Neutron Noise}$$
$$S_{Detected} = \eta_{Scint}\ S_N \pm \sigma_{Detected} \tag{6.4}$$

$$\underline{\textit{Where}}\text{:}\ \sigma_{Detected} = \sqrt{\eta^*_{Scint}\ S^*_N} \tag{6.5}$$

($*$ *Indicates that special units must be used for Dimensional Analysis*)

Note that the units of the noise have changed in this case. Although the signal itself is in units of detected neutron counts, the noise carries the units of (detected unit counts)$^{1/2}$. This is because counts is a dimensional-less unit. Nonetheless, whenever this approximation is allowed by Poisson statistics, the involved variables will be marked by an asterisk sign (*) to avoid confusion with units.[10]

---

[10]Tsoulfanidis, Nicholas, *Measurement and detection of radiation*, pp 57-63.

If the random occurrence of events in this manner was the only source of noise, the system would be known as a Quantum Limited System. For a quantum limited system, as the number of neutrons in the signal increases, the noise grows at a much slower rate. As a consequence, the Signal to Noise Ratio (S/N) increases with a higher neutron fluence:

$$S/N = \frac{S_{Detected}}{\sigma_{Detected}} = \frac{S_{Detected}}{\sqrt{S_{Detected}}} = \sqrt{S_{Detected}} \tag{6.6}$$

Methods for improving neutron statistical noise, especially for a quantum limited system, are discussed in section 9.2.1 of this report.

6.2. Neutron Scintillator

The gain of a scintillator ($_{GSCINT}$), is the number of visible photons per detected radiation event . The fraction of thermal neutrons incident on the scintillator screen which interact with it is known as the detector efficiency (η_{Scint}).

$$Neutron\ To\ Photon\ Gain = G_{Scint} \pm \sigma_{SCINT}$$

Like neutron detection, light emission from a phosphor is also a random event, and Poison statistics dictates that the scintillator will a contribute a statistical noise ($\sigma_{Scint\_Statistical}$) equal to the square root of the number of photons given off per neutron event. In addition, the scintillator will have a fixed pattern noise ($\sigma_{Scint\_Pattern}$) due to irregularities and grain boundaries in the phosphor detector material. Some of these pattern noise can be corrected with a flat field correction, discussed in section 1.4.3 of this report. The scintillator noise (σ_{Scint}) becomes:

$$\underline{WHERE}: \quad \sigma_{Scint} = \sqrt{\sigma^2_{Scint\ Statistical} + \sigma^2_{Scint\ Pattern}} = \sqrt{G^*_{Scint} + \sigma^2_{Scint\ Pattern}} \tag{6.7}$$

($*$ *Indicates that special units must be used for Dimensional Analysis*)

Note that the scintillator statistical noise ($\sigma_{Scint\_Statistical}=(_{GSCINT})^{1/2}$) is very small compared to the signal for our system because the scintillator gain is very large ($_{GSCINT} > 10^4$). However, the term will be kept in our equations to show the effect we could expect of selecting a scintillator

screen that has a lower gain. The scintillator noise is dependent on the neutron event noises in that a neutron event must occur before scintillator noise becomes evident. In every other sense, they are independent, and their total noise (σ_{NT}') can be approximated by the sum in quadrature of the individual noises. The new signal (S_N') due to neutron events converted to photons, emitted from the scintillator screen becomes:

$$Photon\ Signal_{Scintillator} = (Detected\ Neutron\ Signal) * (Gain_{Scint}) \tag{6.8}$$

$$S_N' = (S_N \pm \sigma_N) * (G_{Scint} \pm \sigma_{Scint}) \approx G_{Scint}\, S_N \pm \sigma_N' \tag{6.9}$$

$$S_N' = G_{Scint}\, S_N \pm \sigma_N' \tag{6.10}$$

$$\underline{where}:\quad \sigma_N' \approx \sqrt{G_{Scint}^2\, \sigma_N^2 + S_N^2\, \sigma_{Scint}^2} \tag{6.11}$$

(* *Indicates that special units must be used for Dimensional Analysis*)

For scintillator screens based on a granular phophor, the light is given off in a normal distribution with circular pattern. In our case, this distribution is a peak with a 100 μm full width, half maximum (FWHM).[11] This will vary due to the thickness of the phosphor scintillator screen, depending on where the event occurs within the screen. If the screen is relatively thick compared to degree with which the light spreads, light spots with a variation in the full width, half maximum will be observed.

6.3. Optical System

There will be a significant loss of signal from the scintillator screen to the photon detector in our system. This will be due to two main effects. The first effect is that only a percentage of light will be captured by our lens. The second effect is due to a loss of light transmitted through the lens.

---

[11]Spowart, "Optimising neutron scintillators for neutron radiography", pp 3-11.

When a neutron event occurs, light is given off from an area a few microns across in our scintillator screen. Therefore, this can effectively be modeled as a point source. The fraction, η_Ω, of light that the lens will receive of the total light given off is equal to the solid angle that the lens subtends.

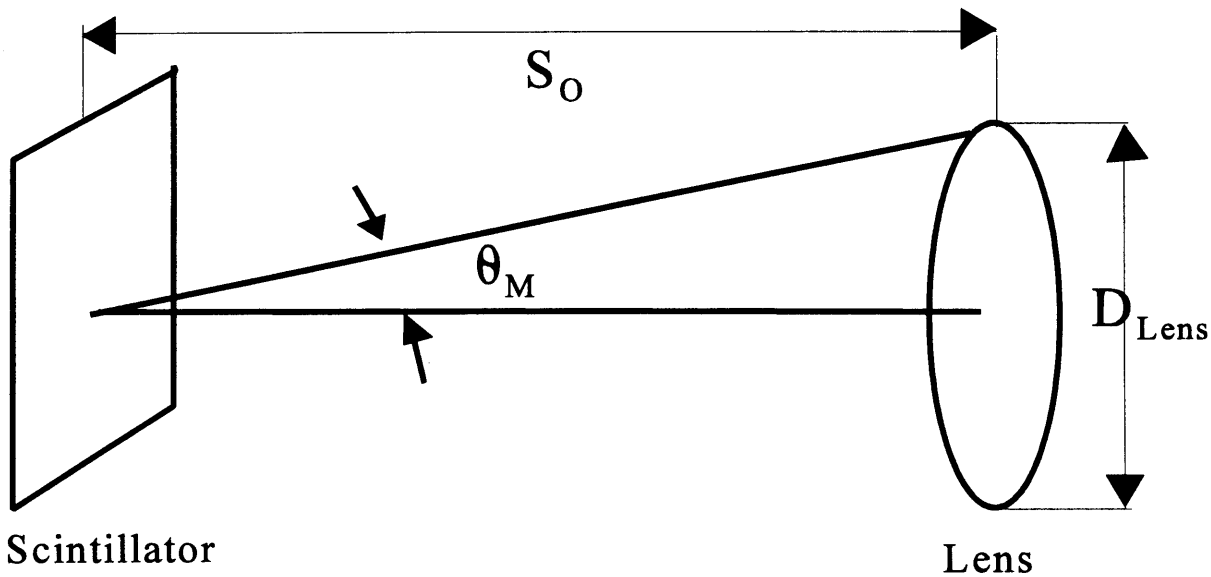

Figure 6.1: Angle Subtended by Lens

For scintillator phosphors, light is not isotropically emitted from the screen, but rather is proportional to cos θ [Lambertion radiator]. For such a light source, the amount of light surviving (η_Ω) is equal to:

$$\eta_\Omega = k \int_0^{\theta_m} \cos\theta \, d\cos\theta = \frac{k\,(1 - \cos^2\theta_M)}{2} = \frac{k \sin^2\theta_M}{2} \qquad \textbf{(6.12)}$$

where k is a normalization constant. If the light is isotropically emitted over the full $\Omega=4\pi$, at most, only half of the light will end up on the side of the scintillator screen with the lens, making k=1. However, it is possible to capture some of the light emitted towards the side opposite of the lens by using a reflective surface that redirects the light back to the lens. In the theoretical case of a perfect reflector, and an infinite size lens, the efficiency for the system (η_Ω) approaches 1, and k=2. Because of internal attenuation within the scintillator screen, it is impossible to achieve the full gain of this reflection. It is interesting to note that the light emission from the screen is slightly forward biased, and therefore not isotropic.[12]

[12]Spowart, "Optimising neutron scintillators for neutron radiography" (sic), pp 3-11.

In terms of the lens diameter (D) and the object distance (S_O), this equation becomes:

$$\eta_\Omega = \frac{k\ D^2}{2\ (4\ S_O^2 + D^2)} \tag{6.13}$$

If the lens diameter (D) is much smaller than the object length (S_O), this equation simplifies to:

$$\eta_\Omega \approx \frac{k\ D^2}{8\ S_O^2} \tag{6.14}$$

As discussed in section 5.3.2, lenses are characterized by f, their focal length and F, the ratio between their focal length (f) and the lens diameter (D). Thus, η_Ω becomes:

$$\eta_\Omega = \frac{k\ f^2}{8\ F^2\ S_O^2} \tag{6.15}$$

The fraction of light that is collected can be written in terms of the minification by using the results of equation 5.4, page 34:

$$\eta_\Omega = \frac{k}{8\ F^2\ (m+1)^2} \tag{6.16}$$

The object distance was varied under our experiments to test different combination of light-loss and minification.

The second effect is that only a percentage of the light that is captured by the lens will survive to the focal area. One reason light is not transmitted is that the lens has internal absorption and surface reflection losses. The percentage of light that survives this loss is measured by an optical efficiency, η_{Lens}. The total number of photons released from the scintillator screen for each neutron event, a fraction of light will be collected a single pixel due to a neutron event (β_{Pixel}). The signal (S_N''), in photons, after the losses due to the optical system is:

$$S_N^{//} = \eta_\Omega \, \eta_{Lens} \, \beta_{Pixel} \, (S_N^{/} \pm \sigma_N^{/})$$

$$S_N^{//} = \eta_\Omega \, \eta_{Lens} \, \beta_{Pixel} \, G_{Scint} \, S_N \pm \sigma_N^{//} \tag{6.17}$$

$$\underline{where}: \quad \sigma_N^{//} = (\eta_\Omega \, \eta_{Lens}) \, \sigma_N^{/}$$

$$= \eta_\Omega \, \eta_{Lens} \, \beta_{Pixel} \sqrt{G_{Scint}^2 \, S_N^* + S_N^2 \, \sigma_{Scint}^2} \tag{6.18}$$

($*$ *Indicates that special units must be used for Dimensional Analysis*)

An optical system which consists of a lens, properly focused, does not significantly contribute to the S/N ratio, because it affects both the signal and the noise together in the same amount.

It is possible to add a light intensifier to the optical system to boost the signal from the neutron scintillator. An intensifier essentially boosts an optical signal by providing a high gain, while maintaining a high spatial resolution. The intensifier may be added before or after the lens, or may warrant a second lens to optimize the intensifier size and output. In may be necessary to add one for some configurations, to make up for the large loss of light due to solid angle losses and lens acceptance angle losses. However, an intensifier will add noise related to the gain of the intensifier-- in the same manner as the scintillator. Its effect on the system noise will depend on how it mates to the lens system being used.

6.4. CCD Detector

The CCD will convert the light signal, from the optical system, to an electrical signal, of electrons stored in a capacitor well. On a CCD chip, there are is an array of capacitor wells, known as pixels. The gain of the CCD, G_{CCD}, is that number of electrons produced per incident photon. The neutron contrast signal ($S_{Contrast}'''$), in terms of electrons in a CCD well, becomes:

$$S_N^{///} = G_{CCD} \, S_N^{//}$$

$$S_N^{///} = G_{CCD} \, [\eta_\Omega \, \eta_{Lens} \beta_{Pixel} \, G_{Scint} \, S_N] \pm \sigma_N^{///} \tag{6.19}$$

$$\underline{where}: \quad \sigma_N^{///} = (G_{CCD})\ \sigma_N^{//}$$

$$= G_{CCD}\ \eta_\Omega\ \eta_{Lens}\ \beta_{Pixel} \sqrt{G_{Scint}^2\ S_N^*\ +\ S_N^2\ \sigma_{Scint}^2} \tag{6.20}$$

($*$ *Indicates that special units must be used for Dimensional Analysis*)

At the current state of technology, the most limiting sources of noise are the read noise and dark current in a CCD. The CCD chip has been designed with an increasing concern given to reducing its noise. A CCD chip is an array of capacitor wells in which elections from a photon to election conversion are stored. There are noises associated with the photon to electron conversion, the number of electrons in the well before the exposure was taken, the number of electrons that leak into the well during the exposure time, and the noise added to the system by analog calculations, and analog to digital conversions.

Fundamentally, the noise associated with sophisticated electronic components such as a CCD or an image intensifiers is limited by the state of technology. Luckily, these optical detection systems are being used in so many different applications that a very strong consumer market has developed around them. As a result, the state of the technology both in the design and manufacture of such components is growing at a remarkable rate. As the technology associated with image intensifiers and CCDs grows, the components signal to noise ratio increases.

6.4.1. Detector Offset and Offset Noise: "Read Noise"

Before an exposure, each pixel is "cleaned", removing any electrons in the capacitor well. However, a few electrons are left in the well after each clean. If a multiple exposures are taken, it is seen that there is a variance on the number of electrons left in the well, and that this noise follows a normal distribution. This is known as read noise:

$$\begin{aligned} \textit{Offset Signal} &= S_{Read} = K_{Read} \\ \textit{Offset Noise} &= \sigma_{Read} \end{aligned} \tag{6.21}$$

6.4.2. Detector Leakage and Leakage Noise: "Dark Current"

Capacitors leak current. As electrons leak into the capacitor well from the surrounding silicon, they add a signal known as dark current. Again, if multiple exposures are taken under

identical conditions, it is seen that there is a variance in the number of electrons that leaked into the well. It is known that the process of electrons leaking into the well is a random event, and is governed by Poison Statistics.

$$Dark\ Current\ Signal = S_{DC} = K_{DC}\ (t)$$

$$Dark\ Current\ Noise = \sigma_{DC} = \sqrt{Signal_{Dark\ Current}} = \sqrt{K^{*}_{DC}\ t^{*}} \qquad \textbf{(6.22)}$$

($*$ *Indicates that special units must be used for Dimensional Analysis*)

6.4.3. Detector Array Noise: "Flat Field" Noise

To further complicate the noise associated with the detector, each pixel responds slightly differently. Note that typical CCD specifications are statistics which are averaged over all of the pixels. We found a significant variance in response between pixels in an array due to statistical variation in manufacturing control processes and position on chip. For example, a voltage drop occurs across the pixels of a chip during operation resulting in slight variations in signals. In addition, due the way pixel information is read and processed, certain pixels will remain on chip longer than others. A pixel pattern noise is create that results from differences in pixel light collection areas, pixel detection efficiency (number of electrons produced per incident photon), dark current rates (K_{DC}), and offset signal (read noise, and the variance in read noise). Each pixel must be individually measured and characterized. This can be quite complicated, because CCD detector arrays are large, and each pixel must be corrected individually. The aggregate signal of the CCD, then will suffer a noise associated with the differences in the detector array, or array noise.

This noise can be removed by treating each pixel individually for noise reduction (dark current and read noise), and then normalizing the response output of each detector based on its "flat field" response. A "flat field" response exposes all pixels to the same level of radiation. Because each pixel will respond differently, a correction factor is assigned to each pixel based on the response of each pixel after a correction for noise is made..

There is also a pattern noise associated with the neutron beam stemming from uneven distribution of neutrons. For example, a neutron beam from a low fluence accelerator source will closely resemble a flashlight beam in a dark room. There will be a bright center region, with an intensity which falls off radially. Again, this noise can be removed by normalizing the pixel array after it has been illuminated by this beam to correct for the beam's uneven distribution. The normalizing constants can then be used to correct images taken with the same non-uniform light (beam) source..

6.5. Signal Conditioning: Analog Signal Processing

The CCD chip has been designed with an increasing concern given to improving the design of the individual pixel's capacitor wells. This is because a significant number of electrons remain in the well after the pixel has been "cleaned" (pixel offset, or read noise), and a significant number of electrons leak into the well during the exposure time (dark current).

To find the signal associated with the neutron events in each pixel detector, all other signals must be removed. Because the signal associated with the neutron event will be different with each pixel, each must be analyzed individually. For example, the analog signal from each pixel contains the following components:

Total Signal = Neutron Signal + Dark Current Signal + Offset Signal ± TotalNoise

$$S_{Total} = S_N^{///} + S_{DC} + S_{Read} \pm \sigma_{Total} \tag{6.23}$$

$$\underline{where}: \quad \sigma_{Total} = \sqrt{(\sigma_N^{///})^2 + \sigma_{DC}^2 + \sigma_{Read}^2}$$

$$= \sqrt{(\sigma_N^{///})^2 + K_{DC}^* \, t^* + \sigma_{Read}^2}$$

$$= \sqrt{(G_{CCD}\, \eta_\Omega\, \eta_{Lens} \beta_{Pixel})^2 \, (G_{Scint}^2 \, S_N^* + S_N^2 \, \sigma_{Scint}^2) + K_{DC}^* \, t^* + \sigma_{Read}^2} \tag{6.24}$$

(* *Indicates that special units must be used for Dimensional Analysis*)

It should be noticed that there a number of ways to process the signal (S_N') to remove the $\text{Signal}_{\text{Dark Current}}$ and $\text{Signal}_{\text{Pixel Offset}}$ from S_N'. The advantage to processing the signal digitally, is once the signal is digitized, the noise can associated with many calculations can be removed. Both analog and digital processing can be built into a chip, which is generally less expensive than digital processing on a computer, especially for parallel processes. However, a tradeoff is that once these processes are built into a chip, they can only be changed to a limited extent. Thus; the user may lose a degree of flexibility.

On our system, the offset signal is removed off chip by a analog process known as double correlated sampling. Each pixel is read once for its signal. The pixel is cleaned leaving only the natural pixel offset. The pixel is then read again to and this is subtracted from its signal, removing the offset signal. However, there is a variance associated with the offset of each pixel, known as the read noise, which is not removed by this double correlated sampling. The signal becomes:

$$S'_{Total} = S_{Total} - S_{Read} = S'''_N + S_{DC} \pm \sigma'_{Total} \tag{6.25}$$

$$\underline{where}: \quad \sigma'_{Total} = \sigma_{Total} = \sqrt{(G_{CCD}\eta_{\Omega}\eta_{Lens}\beta_{Pixel})^2(G^2_{Scint}S^*_N + S^2_N\,\sigma^2_{Scint}) + K^*_{DC}\,t^* + \sigma^2_{Read}} \tag{6.26}$$

($*$ *Indicates that special units must be used for Dimensional Analysis*)

6.6. Signal Conditioning: Analog to Digital Conversion (A/D)

In our system, the analog data is now converted to a digital signal. The designer of the system must choose the number of significant bits to be used in the system. There is a tradeoff between the increased memory and time for each calculation for pixel values converted with more significant digits, and the increased accuracy that may accompany pixel values converted with more significant digits. Fundamentally, the sensitivity of the CCD chip will determine how accurate the A/D can be. For instance, if the analog signal is converted to a 16 bit number, when the CCD only has 8 bit sensitivity, the last 8 bits will simply be noise, and will not increase the system accuracy.

The analog voltage signal from the CCD will be converted to number of counts. The number of counts per electron is a system characteristic known as the gain ($G_{A/D} \pm \sigma_{A/D}$). If the A/D dynamic range is too small, the A/D will add a noise ($\sigma_{Round\ Off}$) to the system by introducing a roundoff error in its calculations. The designer must also choose proper values for the minimum and maximum voltages his A/D will work between to ensure that he/she is making the best possible use of the dynamic range of his system, while minimizing A/D noise.

The number of electrons per A/D count is the A/D Gain ($G_{A/D}$). The signal (S''_{Total}), in A/D counts becomes:

$$S''_{Total} = (G_{A/D} \pm \sigma_{A/D})\,(S'_{Total} - S_{Read} \pm \sigma_{Total}) = G_{A/D}\,(S'''_N + S_{DC}) \pm \sigma''_{Total} \tag{6.28}$$

$$\underline{WHERE}: \quad \sigma''_{Total} = \sqrt{G^2_{A/D}\,\sigma_{Total}{}^2 + (S'_N + S_{DC})^2\,\sigma^2_{A/D} + \sigma^2_{Round\ Off}} \tag{6.27}$$

($*$ *Indicates that special units must be used for Dimensional Analysis*)

If the dynamic range for the A/D is chosen well, the A/D round-off noise ($\sigma_{Round\ Off}$) is significantly smaller than the other sources of noise in our system. If the deviation in the gain ($\sigma_{A/D}$) is also insignificant, then the overall system noise becomes:

$$\sigma''_{Total} \approx G_{A/D}\,\sigma_{Total} \tag{6.29}$$

6.7. Signal Conditioning: Digital Signal Processing

Next, the signal from the Dark Current, the electrons that leak into the well, must be removed. Because dark current shows a reliable linear dependence with time, it is possible to remove the dark current by subtracting from each pixel an exposure taken where no light is allowed into the camera, and the time of exposure is identical with the first picture. It is also possible to generate a mathematical model for each pixel, of the time dependence dark current, and subtract it from the signal of each pixel. Both techniques are susceptible to changing camera characteristics (such as temperature) between the two exposures. The signal due to Neutrons ($S_{Neutron}$), in A/D Counts, becomes:

$$\begin{aligned} S_{Neutron} &= S''_{Total} - G_{A/D}\, S_{DC} = G_{A/D}\, S'''_{N} \pm \sigma_{Neutron} \\ &= G_{A/D}\, G_{CCD}\, \eta_{\Omega}\, \eta_{Lens}\, \beta_{Pixel}\, G_{Scint}\, S_{N} \pm \sigma_{Neutron} \end{aligned} \tag{6.30}$$

$$\underline{WHERE}: \quad \sigma_{Neutron} = \sigma''_{Total} = \sqrt{G^2_{A/D}\, \sigma_{Total}{}^2 + (S'_N + S_{DC})^2\, \sigma^2_{A/D} + \sigma^2_{Round\ Off}} \tag{6.31}$$

($*$ *Indicates that special units must be used for Dimensional Analysis*)

Although the signal of the neutrons is recovered, there are many sources of noise in the system that may mask the true signal. The system must be optimized by reducing the noise well below the Neutron signal.

6.8. Other Sources of Noise

So far, our discussion of noise has only included noise associated with the neutron signal. However, there are two other possible sources of noise which may enter our system. The first is a scintillator response to unwanted forms of radiation, such as gamma rays, fast neutrons or cosmic rays. The second is that the CCD may show a direct response to the radiation, giving us another false signal.

An accelerator based neutron generator will produce a number of different types of radiation. As the target and beam undergo nuclear reactions, more gamma rays are given off, in addition to fast neutrons. Many of the fast neutrons are slowed, and many of the gamma rays are attenuated before they reach the scintillator and CCD but a number of each survives. In addition, there will be background radiation in our experimental vault due to other sources of radiation and

cosmic rays.

The scintillator's response to unwanted forms of radiation can be quite large. Granular Li^6 neutron detectors will produce a significant response to x-rays, depending on the spectrum.[13] Although the scintillator has a much higher cross-section for thermal neutrons than for either fast neutrons, gamma rays or cosmic rays, these interactions can not be neglected. One reason is that the output response to the higher energy radiation can be quite large, another reason is that the there may be a reasonably strong fluence of these other particles. It is difficult to shield the scintillator from the unwanted radiation without reducing the thermal flux of neutrons. Even if the signal can be subtracted from our system by careful calibration, it is very difficult to separate this new source of noise ($\sigma_{Scint\ Rad}$) from our system:

$$\sigma_{Scint\ Rad} = \sqrt{\sigma_{\gamma}^2 + \sigma_{Cosmic\ Ray}^2 + \sigma_{Fast\ N}^2} \tag{6.32}$$

This makes the noise of our scintillator equal to:

$$\sigma_{Scint} = \sqrt{\sigma_{Scint\ Statistical}^2 + \sigma_{Scint\ Pattern}^2 + \sigma_{Scint\ Rad}^2} = \sqrt{G_{Scint}^{*} + \sigma_{Scint\ Pattern}^2 + \sigma_{Scint\ Rad}^2} \tag{6.33}$$

($*$ *Indicates that special units must be used for Dimensional Analysis*)

Another significant source of noise comes from the exposure of the CCD chip to direct radiation, such as x-rays, neutron radiation or cosmic rays.[14]

These are not the only reactions possible. There are also scattering events that could occur. For instance, the neutron could collide with a Si^{28} atom and transfer energy to the target nuclei by the equation:

$$E_{max} = E_o\ (1 - \alpha)$$

$$\underline{where}\ \alpha = \frac{A - 1}{A + 1} \tag{6.34}$$

A = atomic weight of target nucleus (amu)
E_o = Initial energy of neutron (MeV)
E_{max} = Maximum energy transferred to target nucleus (MeV)

---

[13]Spowart, "Measurement of the Gamma Sensitivity of Granular and Glass Neutron Scintillators and Films", pp 1-6.

[14]Ziegler, J. F. IBM Experiments in Soft Fails in Computer Electronics. IBM Journal of Research and Development. May 1995. pp. 3

In particular, particle collisions with neutrons or cosmic rays, and radiation absorption by silicon on the CCD chip can deposit a large amount of energy on chip. Many of these reactions send charged particles through the silicon. These charge particles travel only a short distance in the silicon before being stopped, and result in a large amount of energy being deposited in a very short distance. The kinetic energy of the particles, in part, is transformed into localized ionization and as a results in a large collection of charge within the capacitor wells. Once this energy is transferred, the Si atom could recoil through the Silicon matrix depositing energy along its path.[15]

This additional CCD signal ($S_{CCD\ Rad}$) and noise ($\sigma_{CCD\ Rad}$) can be largely removed by shielding the camera well. In our system, a mirror is used so that the camera can be placed out of the direct line of radiation, and into an area of higher shielding. Lead bricks and cadmium are used as shielding. Radiation noise increases the noise in the CCD before the A/D conversion. The total noise (σ_{Total}) before the A/D conversion becomes:

$$\sigma_{Total} = \sqrt{(G_{CCD}\eta_{\Omega}\ \eta_{Lens}\beta_{Pixel})^2(G^2_{Scint}S^*_N + S^2_N\ \sigma^2_{Scint}) + K^*_{DC}\ t^* + \sigma^2_{Read} + \sigma^2_{CCD\ Rad}} \tag{6.34}$$

($*$ *Indicates that special units must be used for Dimensional Analysis*)

6.9. Contrast

A more useful measure of our system can be found by considering the contrast between what we are imaging and the substrate from which we wish to distinguish. Assume that we are imaging a block of uniform thickness, x, that has a linear neutron attenuation coefficient, μ_X. The detected neutron signal from this material (S_X) at the scintillator screen becomes:

$$S_X = \eta_{Scint}\ \varphi_N\ t\ e^{-(\mu_X)\ X} \pm \sigma_X \tag{6.35}$$

$$\underline{WHERE}: \quad \sigma_X = \sqrt{S_X} \tag{6.36}$$

[15]Letaw, John R. and Normand, E. "Guidelines for Predicting Single Event Upsets in Neutron Environments." IEEE Transactions on Nuclear Science. Vol. 38, No. 6; Dec 1991. pp. 1500-1505.

Now we place a thin strip of a different material, with a thickness y and a neutron attenuation coefficient, $_{\mu Y}$ (representing corrosion), in front of part of the uniform block. The neutron signal at the scintillator screen behind the block with the additional material is:

$$S_Y = \eta_{Scint}\ \varphi_N\ e^{-(\mu_X)\ X} e^{-(\mu_Y)\ Y}\ (t) \pm \sigma_Y \tag{6.37}$$

$$\underline{WHERE}: \quad \sigma_Y = \sqrt{S_Y} \tag{6.38}$$

The contrast signal is the difference between the two different areas:

$$\begin{aligned} S_{Contrast} &= S_X - S_Y = \eta_{Scint}\ \varphi_N\ e^{-(\mu_X)\ X}\ (1 - e^{-(\mu_Y)\ Y})\ (t) \pm \sigma_{Contrast} \\ &= \eta_{Scint}\ [\eta_{Target}\ \eta_{Mod}\ I_D]\ e^{-(\mu_N)\ x}\ (1 - e^{-(\mu_Y)\ Y})\ (t) \pm \sigma_{Contrast} \end{aligned} \tag{6.39}$$

$$\underline{WHERE}: \quad \sigma_{Contrast} = \sqrt{\sigma_X^2 + \sigma_Y^2} = \sqrt{[\eta_{Scint}\ \varphi_N\ e^{-(\mu_X)\ X}\ (t)]\ (1 + e^{-(\mu_Y)\ Y})} \tag{6.40}$$

The S/N relationship of the contrast signal is a very accurate measure of the effectiveness of our system. The contrast effect ($\varepsilon_{Contrast}$) on the signal to noise for the detection can be derived from this relationship:

$$\begin{aligned} \underline{THEREFORE}: \quad S/N_{Contrast} &= \sqrt{[\eta_{Scint}\ \varphi_N\ e^{-(\mu_X)\ X}\ (t)]\ \frac{(1 - e^{-(\mu_Y)\ Y})^2}{(1 + e^{-(\mu_Y)\ Y})}} \\ &= \varepsilon_{Contrast} \sqrt{\eta_{Scint}\ \varphi_N\ e^{-(\mu_X)\ X}\ (t)} \end{aligned} \tag{6.41}$$

$$\underline{WHERE}: \quad \varepsilon_{Contrast} = \frac{(1 - e^{-(\mu_Y)\ Y})^2}{1 + e^{-(\mu_Y)\ Y}} \tag{6.42}$$

For a very high contrast system, the contrast effect ($\varepsilon_{Contrast}$) approaches 1. For this to happen, the criterion, $\mu_Y Y >> 1$, must be met. The result is that contrast signal to noise ($S/N_{Contrast}$) approaches the system signal to noise (S/N_N). Another result is that the saturation criterion, the point for which the contrast signal to noise is within 1% of the system signal to noise, can be derived. For this to happen the contrast ($\varepsilon_{Contrast}$) must be:

$$\varepsilon_{Contrast} = (.99) = \frac{1 - e^{-(\mu_Y)\,Y}}{\sqrt{1 + e^{-(\mu_Y)\,Y}}} \tag{6.43}$$

From this, a relationship between the attenuation coefficient (μ_Y) and thickness (Y) is:

$$(\mu_Y)\ Y = -\ln\frac{2+\varepsilon^2_{Contrast} - \sqrt{8\ \varepsilon^2_{Contrast}+\varepsilon^4_{Contrast}}}{2} = -\ln\left(\frac{2 + (.99)^2 - \sqrt{8\ (.99)^2 + (.99)^4}}{2}\right) \approx 5 \tag{6.44}$$

The linear attenuation coefficient for thermal neutrons for aluminum is .0861 (1/cm). The corresponding saturation thickness for aluminum is 58.2 (cm). In comparison, the linear attenuation coefficient for aluminum hydroxide, $Al(OH)_3$ is 2.4 (1/cm). The corresponding thickness for $Al(OH)_3$ is 2.1 (cm). This shows that the huge difference in contrast that a thermal neutron imaging system would have if it were used to detect aluminum hydroxide corrosion products in aluminum.

For the case when $\mu_Y Y << 1$, the contrast effect can be simplified:

$$\varepsilon_{Contrast} = \frac{1 - e^{-(\mu_Y)\,Y}}{\sqrt{1 + e^{-(\mu_Y)\,Y}}} \approx \frac{1-(1-\mu_Y\ Y)}{\sqrt{1+(1 - \mu_Y\ Y)}} \approx \frac{\mu_Y\ Y}{\sqrt{2 - \mu_Y\ Y}} \approx \frac{\mu_Y\ Y}{\sqrt{2}} \tag{6.45}$$

For example, the greatest possible contrast effect ($\varepsilon_{Contrast}$) that a 100 μm thick area of $Al(OH)_3$ ($\mu_Y Y = .024$) could have with a thermal neutron imaging device would be 1.7%. In other words, the system S/N would be have to be 59 times more sensitive then the calculated S/N if the contrast effect were not included. This is why it is essential that the contrast effect be taken into account in determining the required S/N of the system.

6.10. Signal and Noise Results

A final signal and noise relationship can be derived from the combinations of the sources of noise discussed in this chapter. The system contrast signal and noise relationships become:

$$S_{Contrast} \equiv G_{A/D} G_{CCD} [G_{Scint} \eta_{\Omega} \eta_{Lens} \eta_{Scint} \beta_{Pixel} \varphi_N \; e^{-(\mu_X)\, X} \; (1 - e^{-(\mu_Y)\, Y}) \; t] \pm \sigma_{Contrast}$$

$$= G_{A/D} G_{CCD} [G_{Scint} \eta_{\Omega} \eta_{Lens} \eta_{Scint} \beta_{Pixel} (\eta_{Target} \eta_{Mod} I_D) \; e^{-(\mu_N)\, x} \; (1 - e^{-(\mu_Y)\, Y}) \; t] \pm \sigma_{Contrast} \tag{6.47}$$

$$\underline{\textit{WHERE}}: \quad \sigma_{Contrast} = \sqrt{\sigma_X^2 + \sigma_Y^2}$$

$$\approx [(G_{A/D} \; G_{CCD} \; \eta_{\Omega} \; \eta_{Lens} \beta_{Pixel})^2 \; ((G_{Scint}^2 \; (S_X^* + S_Y^*)$$

$$+ (S_X^2 + S_Y^2) \; G_{Scint}^* + (S_X^2 + S_Y^2) \; (\sigma_{Scint\ Pattern}^2 + \sigma_{Scint\ Rad}^2))$$

$$+ G_{A/D}^2 \; (K_{DC}^* \; t^* + \sigma_{Read}^2 + \sigma_{CCD\ Rad}^2) + (G_{CCD} \; G_{Scint} \; \eta_{\Omega} \; \eta_{Lens} \beta_{Pixel} \; S_X + K_{DC} \; t)^2 \; \sigma_{A/D}^2 \tag{6.46}$$

$$2 \; \sigma_{Round\ Off}^2 + (G_{CCD} \; G_{Scint} \; \eta_{\Omega} \; \eta_{Lens} \beta_{Pixel} \; S_Y + K_{DC} \; t)^2 \; \sigma_{A/D}^2]^{1/2}$$

($*$ *Indicates that special units must be used for Dimensional Analysis*)

Section 3: Discussion and Conclusions

7. Signal to Noise Optimization

The best measure of the effectiveness of our system is the signal to noise ratio of the contrast signal. The signal to noise of the system is simply the ratio of the desired signal to the system noise:

$$\frac{Signal}{Noise} = \frac{S_{Neutron}}{\sigma_{Neutron}} \tag{7.1}$$

In section 6.10, equations for the relationship for the contrast signal and the noise for our system were derived. It is possible to simplify the noise equation by assuming that the scintillator pattern noise ($\sigma_{\text{Scint Pattern}}$), the scintillator radiation noise ($\sigma_{\text{Scint Radiation}}$), the CCD radiation noise ($\sigma_{\text{CCD Rad}}$) and the A/D conversion noise ($\sigma_{\text{A/D}}$, $\sigma_{\text{Round Off}}$) are very small in comparison to the other terms. This gives us the following relationship:

$$\sigma_{Contrast} = \sqrt{\alpha^2 (G^2_{Scint}(S^*_X + S^*_Y) + (S^2_X + S^2_Y) G^*_{Scint}) + G^2_{A/D}(K^*_{DC}\, t^* + \sigma^2_{Read})} \tag{7.2}$$

($*$ *Indicates that special units must be used for Dimensional Analysis*)

<u>*Where*</u>: $\alpha = G_{A/D} G_{CCD} \eta_{\Omega} \eta_{Lens} \beta_{Pixel}$ (7.3)

If the scintillator gain ($_{\text{GScint}}$) is very large, then:

$$G^2_{Scint}\,(S^*_X + S^*_Y) \gg (S^2_X + S^2_Y)\, G^*_{Scint} \tag{7.4}$$

($*$ *Indicates that special units must be used for Dimensional Analysis*)

This allows us to simplify the noise to:

$$\sigma_{Contrast} = \sqrt{\alpha^2\, G^2_{Scint}\,(S^*_X + S^*_Y) + G^2_{A/D}\,(K^*_{DC}\, t^* + \sigma^2_{Read})} \tag{7.5}$$

($*$ *Indicates that special units must be used for Dimensional Analysis*)

But the neutron fluence of the signal at the scintillator screen (S_X ,S_Y) can be expressed in terms of the time dependent flux allowing us to write:

$$\sigma_{Contrast} = \sqrt{\alpha^2[G_{Scint}^2\ \eta_{Scint}^*\varphi_N^*\ t^* e^{-(\mu_X^*)X^*}(1+e^{-(\mu_Y^*)Y^*})] + G_{A/D}^2(K_{DC}^* t^* + \sigma_{Read}^2)}$$

$$= \sqrt{\alpha^2[G_{Scint}^2\ \eta_{Scint}^*(\eta_{Target}^*\eta_{Mod}^* I_D^*\ t^*)e^{-(\mu_X^*)X^*}(1+e^{-(\mu_Y^*)Y^*})] + G_{A/D}^2(K_{DC}^* t^* + \sigma_{Read}^2)} \quad \textbf{(7.6)}$$

($*$ *Indicates that special units must be used for Dimensional Analysis*)

The expression for the contrast signal to noise becomes:

$$S/N_{Contrast} \approx \frac{\alpha\ G_{Scint}\ \eta_{Scint}\varphi_N\ t\ e^{-(\mu_N)x}(1-e^{-(\mu_Y)Y})}{\sqrt{\alpha^2\ G_{Scint}^2\ [\eta_{Scint}^*\varphi_N^*\ t^* e^{-(\mu_X^*)X^*}(1+e^{-(\mu_Y^*)Y^*})] + G_{A/D}^2(K_{DC}^* t^* + \sigma_{Read}^2)}}$$

$$\approx \frac{\alpha\ G_{Scint}\ \eta_{Scint}\eta_{Target}\eta_{Mod}\ I_D t\ e^{-(\mu_N)x}(1-e^{-(\mu_Y)Y})}{\sqrt{\alpha^2\ G_{Scint}^2\ [\eta_{Scint}^*(\eta_{Target}^*\eta_{Mod}^* I_D^*\ t^*)e^{-(\mu_X^*)X^*}(1+e^{-(\mu_Y^*)Y^*})] + G_{A/D}^2(K_{DC}^* t^* + \sigma_{Read}^2)}} \quad \textbf{(7.7)}$$

($*$ *Indicates that special units must be used for Dimensional Analysis*)

There are a number of ways to increase the S/N. It is possible to buy very high quality, low noise CCD's, reducing the dark current growth rate (K_{DC}), and the read noise (σ_{Read}).

7.1. Measuring the Camera Noise and Gain (K_{DC}, σ_{Read}, and $G_{A/D}$)

The dark current and read noise can be calculated for a particular camera using the following method. After covering the camera so that no light can enter into the system, the signal (dark current and read noise offset) measured as a function of time is simply:

$$\begin{aligned} Signal &= G_{A/D}\ (K_{DC}\ t + K_{Read}) \pm \sigma_{Noise} \\ &= A\ t + B \pm \sigma_{Noise} \end{aligned} \quad \textbf{(7.8)}$$

Performing a linear regression on an individual pixel's data at various exposures lengths will give the slope ($A = G_{A/D} K_{DC}$) and the intercept ($B = G_{A/D} K_{Read}$). The data from our camera is shown below:

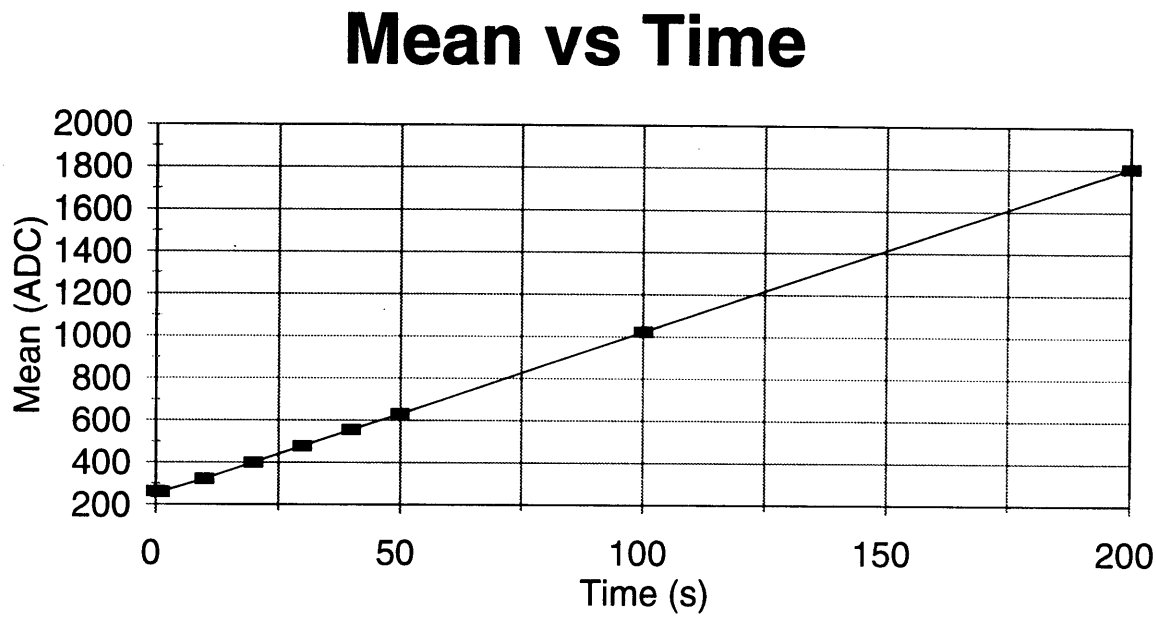

Figure 7.1: Mean vs Time: Noise Measurements for our Camera System

$$Mean = A\ t + B$$

$$\underline{where}: \quad A = G_{A/D}\ K_{DC} \qquad B = G_{A/D}\ K_{Read} \tag{7.9}$$

The noise for this signal is the combination of the following sources of noise:

$$\sigma^2_{Noise} = G^2_{A/D}\ (\sigma^2_{Read\ Noise} + \sigma^2_{Dark\ Current\ Noise} + \sigma^2_{CCD\ Radiation\ Noise}) + (K_{DC}\ t + K_{Read})^2\ \sigma^2_{A/D}$$

$$= G^2_{A/D}\ (K_{DC}\ t^* + \sigma^2_{Read} + \sigma^2_{CCD\ Rad}) + (K_{DC}\ t + K_{Read})^2\ \sigma^2_{A/D} \tag{7.10}$$

($*$ *Indicates that special units must be used for Dimensional Analysis*)

If the CCD camera is well shielded from direct radiation (including cosmic rays), the CCD radiation noise ($\sigma_{CCD\ Rad}$) can be removed from this equation. It will be shown how to measure

the CCD radiation noise ($\sigma_{CCD\ Rad}$) in the next section. The noise data for our camera is shown below:

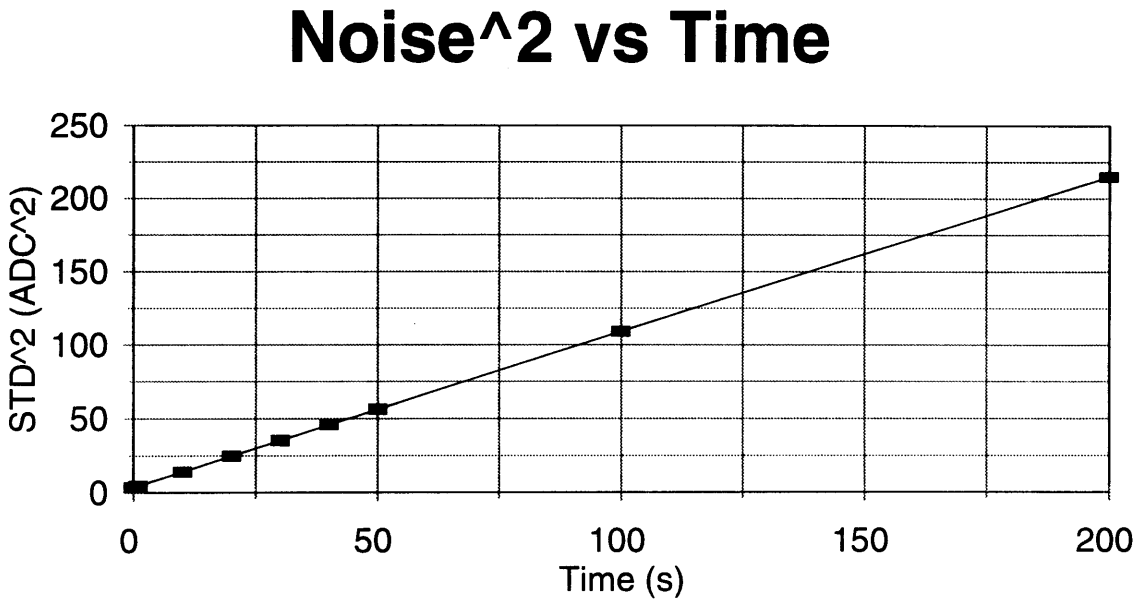

$$\sigma^2 = C\,t^2 + D\,t + E$$

$$\begin{aligned} \underline{where}:\quad C &= K_{DC}^2\,\sigma_{A/D}^2 \\ D &= G_{A/D}^2\,K_{DC} + 2\,K_{DC}\,K_{Read}\,\sigma_{A/D}^2 \\ E &= G_{A/D}^2\,\sigma_{Read}^2 + K_{Read}^2\,\sigma_{A/D}^2 \end{aligned} \tag{7.11}$$

Again, C, D and E can be evaluated using a regression techniques. Using this method, it is now possible to solve these equations for the camera noise and gain characteristics ($G_{A/D}$, K_{DC}, K_{Read}, σ_{Read}, and $\sigma_{A/D}$). Based on this set of data:

$G_{A/D}$	$= 1.27 \times 10^{-1}$	[counts/electron]
K_{DC}	$= 61.3$	[electrons/sec]
K_{Read}	$= 1.94 \times 10^{3}$	[electrons]
σ_{Read}	$= 15.5$	[electrons/STD]
$\sigma_{A/D}$	$= 2.98 \times 10^{-4}$	[(counts/electron)/STD]

Note that our assumption that the gain noise ($\sigma_{A/D}$) is much smaller than our other noise terms is correct. This source of noise can be omitted in our calculations.

A few things must be considered about this technique for measuring the camera characteristics. First, the noise of the camera is highly sensitive to temperature. The dark current doubles every 7° C, and both the read offset and the read noise increase with temperature. (The above measurements were taken with the camera operating at 40^{0} C.) This makes the camera sensitive to operating temperature conditions. Another concern with measuring the noise characteristics in this way is that as previously mentioned, each pixel will have its own noise characteristics (K_{DC}, K_{Read}, σ_{Read}), which can differ significantly from the pixel averaged numbers presented above. The fluctuation from pixel to pixel will become significant in our discussion in the next chapter. The noise of each pixel in the array can be measured using the above technique.

7.2. Measuring Other CCD Characteristics

By adding sources of signal and noise to our camera system, one at a time, we can measure and evaluate its effect on the camera. For example, the next source of noise to measure in this system might be CCD radiation noise ($\sigma_{CCD\ Rad}$).

It should be noted that the radiation noise due to background and cosmic radiation is not insignificant. We found that for long exposures (t > 10 sec) on our CCD, cosmic rays and background radiation would give us erroneous data points if not corrected, even in a well shielded facility without our accelerator running. Direct interaction with cosmic rays would occasionally deposit large amounts of energy in the CCD chip, but such events were easy to find as those affected pixels would have extraordinarily high counts. In this way, the CCD chip was found to fail much like dynamic ram chips have been shown to due to cosmic rays (see section 6.8). When additional sources of radiation are introduced, such as neutrons, the CCD radiation noise ($\sigma_{CCD\ Rad}$) greatly increased. Because of the amount of energy deposited in the affected pixels due to direct radiation affects, the CCD radiation noise ($\sigma_{CCD\ Rad}$) cannot be ignored.

To measure this noise, the camera lens should be covered to block any possible sources of light, repeating the experimental setup used to measure the camera gain and noise. Once the camera system parameters ($G_{A/D}$, K_{DC}, K_{Read}, and σ_{Read}) are known, the camera can be exposed to different levels of radiation to determine the effects on radiation and shielding on the camera and thus measure the CCD radiation noise ($\sigma_{CCD\ Rad}$). We can use this same method of measurement to characterize the other major components of signal and noise in our camera system.

7.3. Optimizing the Camera to Create a Quantum Limited System

Based on our calculations, there will be an exposure time (t), for which the dark current noise is much greater than the read noise:

$$K_{DC}\ (t) \gg \sigma^{2}_{Read} \tag{7.12}$$

If the exposure time is sufficiently long enough to make the read noise insignificant (t < 10 sec for our camera system), we can rewrite the signal to noise ratio in such a way to show that it is proportional to the square-root of the exposure time , the expression for S/N becomes:

$$S/N_{Contrast} \approx \frac{\alpha\, G_{Scint}\, \eta_{Scint}\, \varphi_N\, e^{-(\mu_N)\, x}\, (1 - e^{-(\mu_Y)\, Y})\, \sqrt{t^*}}{\sqrt{\alpha^2\, G^2_{Scint}\, \eta^*_{Scint}\, \varphi^*_N\, e^{-(\mu^*_X)\, X^*}\, (1 + e^{-(\mu^*_Y)\, Y^*}) + K^*_{DC}}}$$

$$\approx \frac{\alpha\, G_{Scint}\, \eta_{Scint}\, \eta_{Target}\, \eta_{Mod}\, I_D\, e^{-(\mu_N)\, x}\, (1 - e^{-(\mu_Y)\, Y})\, \sqrt{t^*}}{\sqrt{\alpha^2\, G^2_{Scint}\, \eta^*_{Scint}\, (\eta^*_{Target}\, \eta^*_{Mod}\, I^*_D)\, e^{-(\mu^*_X) X^*} (1 + e^{-(\mu^*_Y) Y^*}) + K^*_{DC}}} \qquad \textbf{(7.13)}$$

$$= A\, \sqrt{t^*}$$

<u>*Where*</u>: A = *Constant of Proportionality*

($*$ *Indicates that special units must be used for Dimensional Analysis*)

Under these conditions, it should be noted that the signal is growing faster than the noise, so it is desirable to increase the exposure time, if possible and make this condition. The constant of proportionality (A) can be easily calculated from experimental data to determine.

Another way to remove the effect of the read noise is to increase the following system constants (G_{Scint}, $\alpha = G_{A/D}\, G_{CCD}\, \eta_\Omega\, \eta_{Lens}\, \beta_{Pixel}$). This will have the effect of increasing the signal to noise until the following condition is met:

$$\alpha^2\, G^2_{Scint} \eta^*_{Scint} \varphi^*_N e^{-(\mu^*_X) X^*} (1 + e^{-(\mu^*_Y) Y^*})\, t \;\gg\; (K^*_{DC}\, (t^*) + \sigma^2_{Read})$$

$$\alpha^2\, G^2_{Scint} \eta^*_{Scint} \eta^*_{Target} \eta^*_{Mod} I^*_D e^{-(\mu^*_X) X^*} (1 + e^{-(\mu^*_Y) Y^*})\, t \;\gg\; (K^*_{DC}\, (t^*) + \sigma^2_{Read}) \qquad \textbf{(7.14)}$$

($*$ *Indicates that special units must be used for Dimensional Analysis*)

Until this is met, increasing these parameters will have the affect of increasing the signal faster than then noise. Once this condition is met the noise and the signal will increase at the same rate and the S/N will not be affected. In this case, the S/N becomes the same equation derived in section 6.10:

$$S/N_{Contrast} \approx \varepsilon_{Contrast} \sqrt{\eta^*_{Scint}\ \varphi^*_N\ e^{-(\mu^*_X)X^*}\ t^*}$$

$$\approx \varepsilon_{Contrast} \sqrt{\eta^*_{Scint}\ \eta^*_{Target}\ \eta^*_{Mod}\ I^*_D\ e^{-(\mu^*_X)X^*}\ t^*} \qquad \textbf{(6.42)}$$

($*$ *Indicates that special units must be used for Dimensional Analysis*)

$$\underline{\textit{WHERE}}: \quad \varepsilon_{Contrast} = \frac{(1 - e^{-(\mu_Y)\ Y})^2}{1 + e^{-(\mu_Y)\ Y}} \qquad \textbf{(6.43)}$$

The coefficients ($\varepsilon_{Contrast}$, $e^{-\mu X}$, η_{Scint}, φ_N (η_{Target}, η_{Mod}, I_D), and t) also reduced the signal to noise ratio. Unlike the first set of coefficients (G_{CCD}, G_{Scint}, η_Ω, and η_{Lens}), the signal to noise continues to improve with the square root of the second set of coefficients is increased, even after the above mentioned condition is met. This occurs because they are the quantum limits of our system.

If the system is only limited by the neutron statistical noise, it is known as **Quantum Limited**. It becomes obvious that the only way to improve a quantum limited system for a given phantom is to increase the total number of neutrons, known as the **Neutron Fluence**, by either increasing the detected flux at the scintillator screen, or by increasing the exposure time.

The most logical way to improve the signal to noise of our system is to increase the detected neutron fluence. If we are Quantum Limited, this is the only way to improve the S/N. Increasing the neutron fluence as a means to decrease the noise is discussed in Chapter 9.

It is important to see that the signal to noise can be significantly improved with longer exposure times. However, there are limitations and tradeoffs. The first is that the capacitor size of a CCD is finite, and the exposure must be stopped before the capacitor saturates. This limits the length of an exposure because the capacitor "well" is filling with both signal and dark current.

If the exposure time in the above equation is fixed, the signal to noise can be improved by lowering the dark current constant, meaning that the well will fill with a higher percentage of neutron signal before saturating.

One way to lower the dark current is to buy a less noisy CCD, or to reduce the dark current noise of the CCD by cooling it. Because dark current in a CCD is a function of temperature, cooled CCD cameras have a much lower dark current signal, and as a consequence, have a lower dark current noise.

8. Counting Circuits

8.1. Introduction to the Counting Circuit

It has already been shown that a increased time of exposure will yield better S/N ratio. However, a very short exposure could also have a few benefits of its own. If the exposure time was short enough to guarantee that a pixel was hit by at most one neutron, then each neutron event could be independently registered as part of a **Counting Circuit**. If a large number of short exposures were taken as such, the number of neutron events per pixel could be added to form the total image. The advantages of such a system is that it would be limited only by the statistical noise of the detected neutron flux, and therefore be quantum limited.
A counting circuit would have to have a low enough noise to detect a single neutron. Using the results from section 6.10, the signal of a single neutron event (in counts ADC) is:

$$S_{Counting\ Circuit} \equiv G_{A/D} G_{CCD} \beta_{Pixel} G_{Scint} \eta_{\Omega} \eta_{Lens} \pm \sigma_{Counting\ Circuit} \tag{8.1}$$

<u>*Where*</u>: $\sigma_{Counting\ Circuit} = [(G_{A/D}\ G_{CCD}\ \eta_{\Omega}\ \eta_{Lens}\beta_{Pixel})^2\ (G^*_{Scint} + \sigma^2_{Scint\ Pattern} + \sigma^2_{Scint\ Rad})$

$$+ G^2_{A/D}\ (K^*_{DC}\ t^* + \sigma^2_{Read} + \sigma^2_{CCD\ Rad}) + (\ G_{CCD}\ G_{Scint}\ \eta_{\Omega}\ \eta_{Lens}\beta_{Pixel} + K_{DC}\ t)^2\ \sigma^2_{A/D}]^{1/2} \tag{8.2}$$

($*$ *Indicates that special units must be used for Dimensional Analysis*)

There are a number of advantages to using a counting circuit to achieve a quantum limited system. One advantage is that much less expensive CCD camera systems could be used. For example, an exposure could be short enough that the dark current noise was insignificant:

$$K_{DC}\ (t) \ll \sigma^2_{Read} \tag{8.3}$$

If the dark current is no longer a major factor in the system, a cooled CCD camera would become largely unnecessary.[16] Because we do not require a large pixel capacitor well for our exposures, this too is no longer a requirement of our CCD camera. Because images are combined off chip, there is no exposure time limitation associated with finite well capacity.

It is possible to use electronic averaging or counting techniques to further reduce the

---

[16]Kolbe, Turko, Berkely, "Recovery of Very Low Intensity CCD Images From Noise",pp 731 - 733.

noise of our system, and improve the detector resolution, making it easier to design a quantum limited system[17]. A counting circuit can largely remove response associated with the unwanted radiation mentioned in section 6.8. It does this by setting a minimum threshold value and a maximum value for the signal from a pixel ($S_{\text{Counting Circuit}}$) for which a thermal neutron event can occur. If the values are set well, the response to unwanted radiation will largely fall outside of this filter window and only neutron events will be recorded.

A counting circuit used in conjunction with a pulsed neutron source (such as is in use in our system) opens up a number of new possibilities. If the pulsed system has a low duty cycle, then neutron signals are collecting only during the pulse, while dark current and other sources of unwanted signal and noise is accumulating during the entire time. Thus the S/N during a pulse is significantly higher than the time averaged S/N which is collected during the latency period as well during the pulse. It is possible to sync the exposure time of the counting circuit with the neutron pulse, and read the CCD between pulses, then the system would take full advantage of the higher S/N during a pulse.

For example, one source of noise that could be totally eliminated by this timing method would be the scintillator's response to unwanted radiation such as high energy gamma rays and fast neutrons. Immediately after a deuteron pulse strikes the target, a large number of fast neutrons and gamma rays are created. A number of these fast neutrons slow down to thermal energies before they reach the scintillator screen a short time later. By gating the CCD to integrate only after the unwanted fast neutrons and gamma rays have passed, the noise in the system due to these components can be completely removed.

8.1.1. Types of Counting Circuits

The following sections describe counting circuits tested by this project. The counting circuits fall into two separate regimes depending on whether the spatial resolution of the detection system is limited by the CCD detection system, or the scintillation device. A third regime is when the resolution of the CCD detection system is approximately the same as that of the scintillation device.

The ratio between the size of the light release from the scintillator screen per neutron event (object) and the resulting image projected on the pixel (image) is the minification, as defined in section 5.3.2. For a scintillator which is optically coupled to a light detector, the designer can change the relative size of the detector to the scintillator by changing the minification of the system. This gives the experimenter the capability to alter the spatial resolution of the system and in addition, to optimize the counting circuit.

A simple model helps illustrate the difference between these three regimes. After detecting a neutron, the scintillator device gives off a flash of light, that when viewed from a distance, resembles a small area of light. The image of this flash is projected onto the CCD chip using lenses. We will define an image diameter which captures 99% out of the total light

---

[17]Kolbe, Turko; Berkely, "Recovery of Very Low Intensity CCD Images From Noise",pp 731 - 733.

projected onto the CCD from a single event. This diameter (D_{Scint}) is a measure of the projected scintillator's resolution. CCD's are typically laid out in square or hexagonal close-packed arrays. We can model the CCD as a two dimensional array of squares of a given length (L_{Pixel}).

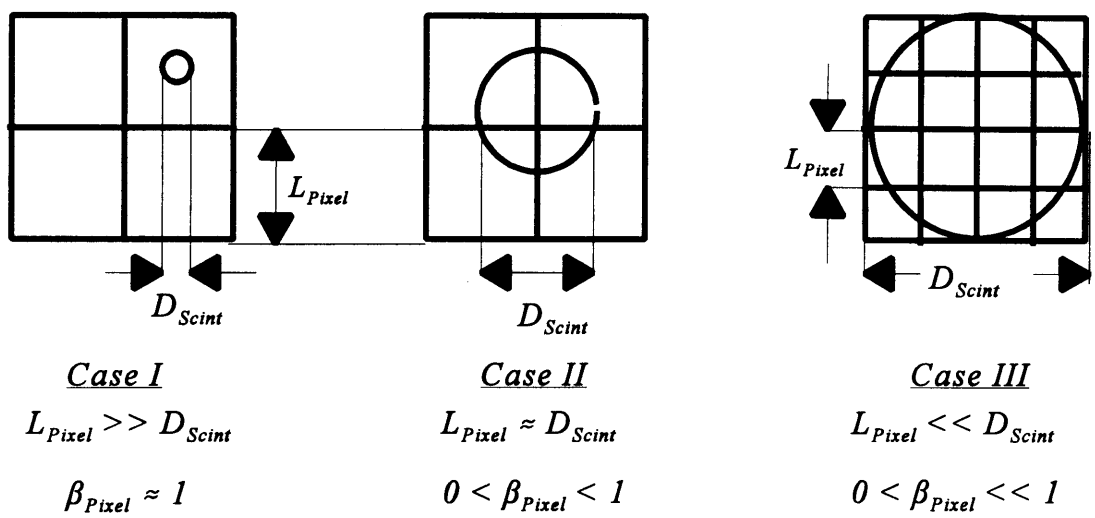

Figure 8.2: Relative Sizes of the Pixel and the Projected Image of a Neutron Event from the Scintillator Screen

If the pixel is larger than the circle of light given off by the scintillator ($L_{Pixel} >> D_{Scint}$), the CCD pixel size limits the resolution of the detection system. In this case, all of the light from a neutron event that is incident on the CCD falls into a single pixel ($\beta_{Pixel} = 1$ for the single affected pixel, and $\beta_{Pixel} = 0$ for all others). If all the light is collected within one pixel for most events, the CCD pixel acts as a single detector system. In this case, each CCD pixel acts independently of the other.

If the pixel size is on the same order of magnitude as the scintillator screen circle, it becomes much more likely that the light collected from a neutron event will be shared by more than one pixel. In this event, the CCD pixel array becomes a redundant detector system. Information from each neutron hit is deposited in multiple pixels.

The extreme case of a redundant detector system is one in which the area of light from the scintillator is much larger than an individual pixel ($L_{Pixel} << D_{Scint}$). In this case, the scintillator screen limits the spatial resolution of the detection system and the light will be distributed over many pixels ($0 < \beta_{Pixel} < 1$ for the effected pixels).

8.1.2. Case I: CCD Limited Spatial Resolution System

A very simple counting circuit could be devised for the case when the spatial resolution of the system is limited by the CCD spatial resolution. In this case, the area of light projected onto the CCD from a neutron event is very small compared the CCD pixel. This means that all of the light from scintillator due to a neutron event that is incident on the CCD will be collected

in a single pixel ($\beta_{Pixel}=1$). A simple thresholding device could be used to check each pixel for neutron events by setting a threshold value for each detector device based on normal background levels. If the detector was over the threshold value, the detector can be assumed to have been hit by a neutron. A maximum value could then be set for a neutron event. If the detector value was greater than this maximum value, it can be assumed that the event was caused by another source of radiation.

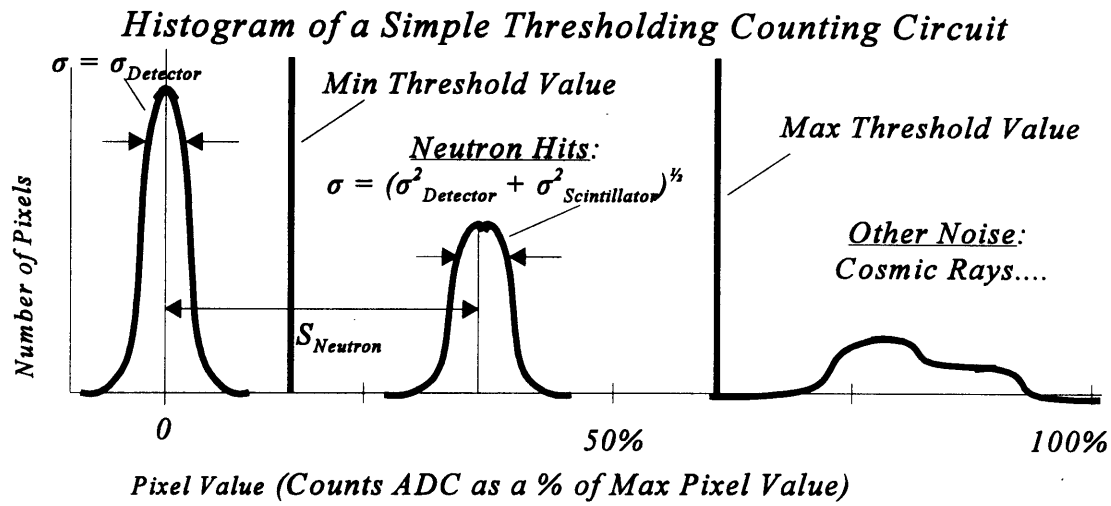

Figure 8.3: Case I: Histogram of a Simple Thresholding Circuit ($L_{Pixel} >> D_{Scint)t}$)

The histogram for Case I shows the distribution of pixel values in a simple thresholding counting circuit. The first peak represents pixels that have not been hit by neutrons ($\beta_{Pixel} = 0$). This peak can be modeled as a normal distribution with a standard deviation (σ) equal to the detector noise ($\sigma_{Detector}$). The second peak represents pixels that have recorded neutron events. Again, this peak can be modeled as a normal distribution with a standard deviation (σ) equal to the summation of the detector noise ($\sigma_{Detector}$) and the scintillator noise ($\sigma_{Scintillator}$). These noises are independent of each other and add in quadrature. The distance between the first and second peak is the average signal due to a neutron event ($S_{Neutron}$) and is controlled by the sensitivity of the detector device to a neutron event. The last peak represents large detector response to unwanted forms of radiation. Two thresholds have been set, representing the minimum and maximum value that a pixel with a neutron event may have. Therefore, any pixel falling within these two values could be recorded as a neutron event, and the rest can be discarded as noise.

It is possible that a single pixel could be "hit" by multiple neutrons. For example, if the exposure time and flux level were such that the 30% of the pixels have recorded a neutron hit, then $((.3)^2)/2 = (4.5\ \%)$ of the pixels would have two neutron events. If the noise was low enough, and the gain high enough (ie: the S/N high enough), then a second peak would appear in the histogram for pixels that have been hit twice. Like the first peak, the standard deviation (σ) would be controlled by the detector and scintillator noises, and the distance between peaks would be controlled by the detector gain. The maximum number of neutron events that can be separated from the noise with certainty on an individual pixel establishes the limit for the neutron fluence for our system. The neutron fluence (controlled by the exposure time and the neutron

flux) would have to be low enough to ensure that there was not a significant number neutron events that were lost due to our inability to separate out these multiple events on a single pixel from noise.

The criteria for use of a simple threshold counting circuit are shown in Figure 8.4. The first criterion requires a detector with a high signal to noise. To distinguish an event, it is necessary to be able to pick out a single pixel that has been hit a neutron event, from those that have not been hit. The signal due to a neutron hit must be large enough and the noise small enough to statistically separate the two. If the scintillator or the detection system is too noisy or the signal due to a neutron event too low, the neutron peak will overlap with the peak from the system background. In other words, overlap will occur if either peak's width increases significantly, or if the distance between the peaks decreases markedly. If the peaks overlap, it will be impossible to detect all the neutrons without getting noise from the system. If the threshold value is set conservatively to remove noise, not all of the events will be recorded. If an attempt is made to include these lost values, random system noise may be recorded as an event.

Criteria for a Simple Threshold Counting Circuit

- Detection of a single neutron event: ($S/N_{Counting\ Circuit} >> 1$)
- A single neutron event must occur within a single pixel ($\beta_{Pixel} = 1$)
- Limits number of neutron events per exposure
- CCD limited resolution ($L_{Pixel} >> D_{Scint}$)
- Requires Multiple exposures

Figure 8.4: Case I-- Criteria for Threshold Counting Circuit

As already discussed, the criteria require that the resolution of the scintillator be much better than the detector array. This can be accomplished with optical coupling or by binning pixels together on the CCD.

Therefore, the efficiency of the simple counting circuit is dependent on (1) minimization of the scintillator and (2) detector system noise (controls the width of the noise peak and the neutron peak), or (3) maximizing the signal due to a neutron event, and thus sensitivity of the detector (controls the spacing between the noise peak and the neutron event peak). This gives the designer of the circuit three independent means to improve the of the counting circuit.

8.1.3. Case II: CCD Resolution Equals Scintillator Resolution

If the CCD spatial resolution is approximately on the same order of magnitude as the scintillator spatial resolution, the system histogram is quite different. It is more likely that the light from a single neutron event will affect multiple pixels, each receiving a fraction of the total light ($\beta_{Pixel} < 1$).

Although the histogram of pixel values our experiment measured for Case II shows a peak for pixels involved in a neutron event, the peak was not be well separated from the peak of unaffected pixel. This is due to a number of reasons: (1) the signal from an affected pixel is much lower because it only collects a fraction of the light (β_{Pixel}), (2) the fraction of light each pixel receives will vary widely, (3) multiple pixels are affected for each event, and (4) there are a

large number of pixels hit with a very low percentage of light ($0 < \beta_{Pixel} << 1$) for each event which blurs the distinction between the two peaks. It should be noted that the upper threshold limit can still be used to remove unwanted radiation and noise that had a high detector response.

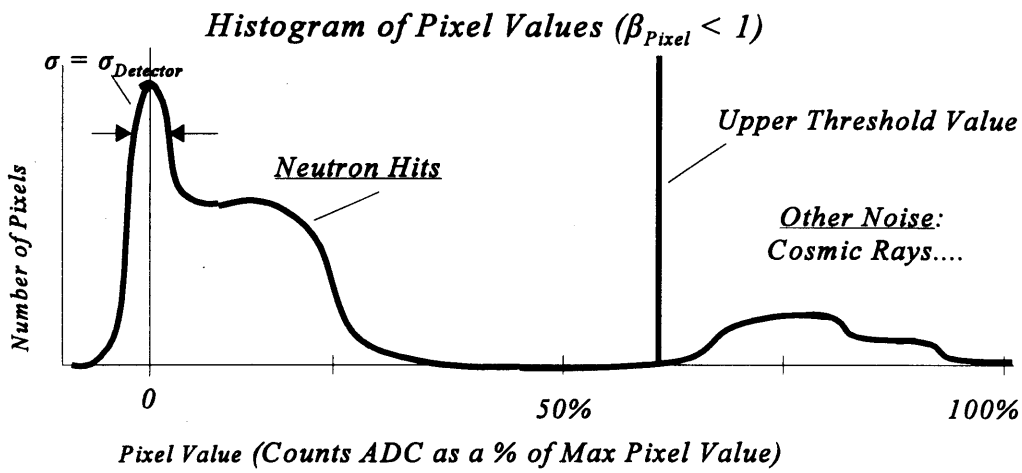

Figure 8.5: Case II: Histogram of a Thresholding Circuit ($L_{Pixel} \approx D_{scin)t}$)

Although it is possible to use a counting circuit to detect neutrons under these conditions, the efficiency of the circuit is much lower than it was in Case I. It becomes difficult to detect neutron events with a simple thresholding technique even with an excellent signal to noise ratio for the system. If multiple pixels are affected by a neutron event, it is difficult to set a threshold value that will guarantee only one pixel is counted per event. An attempt to set a lower thresholding limit either resulted in a neutron events being recorded multiple times or in a number of neutron events simply being discarded with the noise of the system. The first of these options no longer fits the definition of a counting circuit. The second option results in a much lower detection efficiency for the system.

8.1.4. Case III: Scintillator Limited Spatial Resolution System

If the CCD spatial resolution is much greater than the spatial resolution of the scintillator, a different type of counting circuit must be used. In this case, each pixel receives a much smaller fraction of the light incident on the CCD ($0 < \beta_{Pixel} << 1$).

Again, the histogram we measured for this system shows that because the light from each neutron event is spread over multiple pixels setting lower threshold value will give multiple pixels for each event. This makes it possible to design and implement noise filters to remove random noise and CCD response to unwanted radiation. A "bubble-finder" filter was devised to examine adjacent pixels and determine if there was a "hit" that spanned multiple pixels (ie. a "bubble"). This algorithm then calculated the weighted centroid of each bubble and recorded it as a single neutron hit.

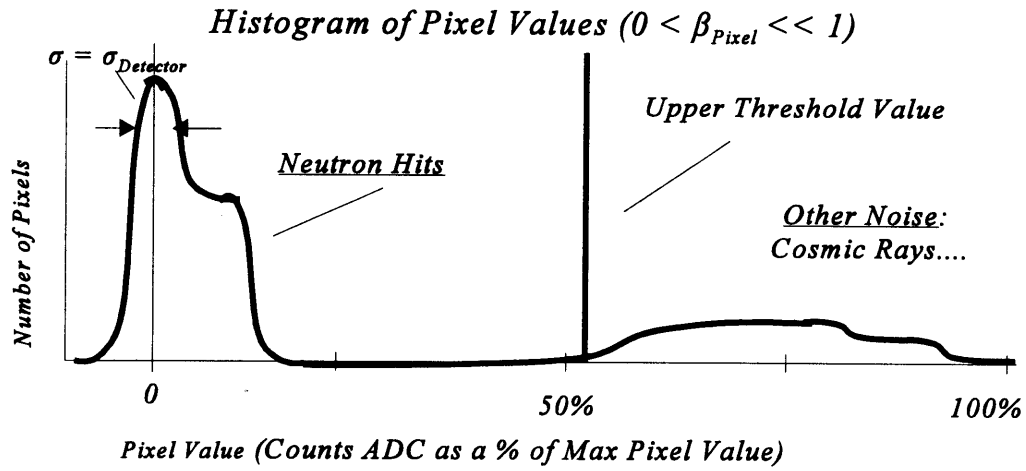

Figure 8.6: Case III: Histogram of a Thresholding Circuit ($L_{Pixel} << D_{scin)t}$)

A separate noise filter was developed to decrease the random noise of the CCD and the increased the reliability of our system in finding neutron events by removing unwanted detector noise. Because the fraction of light collected in each pixel is small ($0 < \beta_{Pixel} << 1$), the signal strength is much lower for this detector collection technique. Therefore, it is critical that the noise of the system be minimized to maintain a reasonable signal to noise.

A number of noise filters were tested to see their effects on removing system noise. The first technique was the already mentioned thresholding techniques. The initial setting of a minimum thresholding value removes much of the unwanted low pixel value noise. If the minimum threshold value is set too high, pixels that collected small fractions of light (low β_{Pixel}) will be discarded, and this may affect the accuracy of the bubble recognition and centroid calculation. By setting a maximum threshold value, we can again discard the unwanted random noise and radiation noise for which our detection system gave a high pixel response.

The next variant of the noise filter was also able to remove noise based on the number of pixels involved in a given "event". Because a neutron event spans multiple pixels, it is possible to distinguish how many pixels were involved in an event. The number of pixels involved in a neutron event gave us another criteria for which we can filter out noise in the system. By only considering those "bubbles" that spanned a set number of pixels (the number of pixels involved in a neutron event could be obtained through calculations or by empirical measurement), random pixel noise had much less of an effect on the system. Thus the improved noise filter drastically decreased the detectors sensitivity to random pixel noise, meaning that a more noisy, lower grade (and therefore cheaper) CCD camera could be used.

The "bubble finder" counting circuit, used in conjunction with the noise filter, was found to be the closest to quantum limited of all the imaging configurations investigated (if we were operating in the Case III regime). The system uses sheer processing power to overcome problems with high noise cameras, low gain systems, and low spatial resolution systems. In addition, the bubble finding filter in some cases improved the resolution of our system beyond the limitations of either the CCD pixel size or the scintillator resolution. The more pixels the

event occurred over, the more accurate the resulting calculation of the centroid. It is possible to obtain a much higher spatial resolution than either that of the CCD or the scintillator screen.

There were disadvantages to using these filters. The largest disadvantage was that it required either a large amount of post-processing of our data, or a relatively expensive dedicated computer board known as a Digital Signal Processor (DSP). The amount of time required increased with the number of exposures, the number of bubbles in the image, the noise of the system, and the size of the image. Thus for very low fluences, and smaller CCD array sizes, it was possible to process the data at the frame rate of our camera on our P-6, 200 MHZ PC.

A second disadvantage was that unlike the Case I simple thresholding counting circuit, the bubble finding routine cannot be designed to handle pixels that were hit with multiple neutron events. Because more pixels are involved per event, the number of pixel hits per frame is drastically reduced, far lower than the simple counting circuit. The lower fluence and high processing power limitations of this system may require multiple cameras imaging smaller areas in parallel for higher neutron flux systems. However, as faster, lower noise, less expensive cameras and more less expensive, more powerful PCS and DSPs become available, these limitations should less restrictive.

8.2. Other Detector Methods

A number of alternative neutron detector methods were investigated. As previously discussed, the goal of the detector is to create a quantum limited, high efficiency system. There are a number of developing technologies that may supplement or replace our current system.

A light intensifier could be used to increase the signal of our system. A light intensifier multiplies the number of photons in a light signal by many orders of magnitude and is capable of maintaining very high spatial resolutions. The gain of a light intensifier can be quite large, boosting the signal many orders of magnitude. This gain comes at a price: the noise contributed by a light intensifier may be much larger than many of the noises discussed in chapter 6. In fact, the light intensifier may become the most significant noise in our system.

Under certain conditions, the light intensifier's noise will not affect the overall signal to noise of the system. For example, if our system is quantum limited before we add the light intensifier, the intensifier is not likely to improve or degrade the system performance.

Under other conditions, the signal to noise will increase dramatically. This is possible, for example, if the addition of a light intensifier brings us closer to a quantum limited system. For example, a light intensifier used in conjunction with a threshold counter would increase the signal due to a neutron event, and thus make it very easy to detect pixels that have been hit with a neutron event from those that have not. Thus a quantum limited counting circuit detector could be made from a lower cost, higher noise CCD.

It is possible that the signal to noise for the system could be decreased with the addition of the light intensifier. This final case is possible if the light intensifier's noise drastically increases the noise of the system.

Another advantage of a light intensifier is that it may be gated with very high time resolution. For a pulsed accelerator source, this can be useful in eliminating unwanted noise that occurs before or after the time that the desired energy neutrons reach the scintillator screen. For

example, it could be gated to remove fast neutrons if one were to image with thermal neutrons, based on time of flight.[18] However, light intensifiers with high spatial resolution and good time resolution can be very expensive. In addition, because the light intensifiers are usually quite small, they will suffer the same optical light loss problems that our CCD did, with the added inconvenience that their photon detection efficiency may be lower than that of a CCD. The few photons that are detected by the light intensifier will be multiplied by a very large gain, entire events may be lost if they don't produce enough photons that survive to be detected by the light intensifier.

There are a number of emerging technologies that neutron imaging techniques may benefit from. For example, the Charge Injection Device (CID) technology or, MOS type CCD devices could one day replace current CCD chips with lower cost, lower noise systems. These could easily be implemented by replacing our current CCD.

Amorphous silicon offers the potential to provide a very large photon detecting device. Such a device would have a much larger surface area than a CCD, and would therefore alleviate many of the problems of light loss caused by the optical light loss due to minification and the need for a bulky optical coupling system. In fact, because the optical efficiency of the system ($\eta_{Optical} = \eta_{\Omega}\, \eta_{Lens}$) would be very close to .5, the signal would be immediately improved by a factor of at least 10^2 in our current system (currently $\eta_{\Omega}\, \eta_{Lens} < .004$). Therefore, such a device could potentially have a much higher signal to noise due to the increased photon signal, making it easier to design a quantum limited detector. Such a device is capable of video frame rates, and would be relatively insensitive to radiation. Current technology appears to be capable of noise levels around 10^3 e/pixel.[19] A neutron event would cause approximately 5×10^4 electrons/pixel with our existing scintillator screen. Because of the large signal and the large pixel size of an amorphous silicon detector, the device would be capable of being used as a counting circuit (Case I).

---

[18]Guzek, J, C. B. Franklyn, G. Pfister, M. C. Steyn, J. I. W. Watterson, A. K. Schatz and U. A. S. Tapper, "The Feasibility of Time of Flight Fast Neutron Radiography"

[19]Street, R, Private Conversations.

9. Optimizing a Quantum Limited Neutron Radiography System

A quantum limited neutron tomography system is solely limited by the statistical noise of neutron detection. In section 7, a relationship has been derived for the S/N of a quantum limited system:

$$S/N_{Contrast} \approx \varepsilon_{Contrast} \sqrt{\eta^*_{Scint}\ \varphi^*_N\ e^{-(\mu^*_X)\ X^*}\ t^*}$$

$$= \varepsilon_{Contrast} \sqrt{\eta^*_{Scint}\ \eta^*_{Target}\ \eta^*_{Mod}\ I^*_D\ e^{-(\mu^*_X)\ X^*}\ t^*} \qquad \textbf{(9.1)}$$

($*$ *Indicates that special units must be used for Dimensional Analysis*)

This equation shows that there are many ways to increase the S/N of a quantum limited system. Not all of the techniques to improve such a system are suggested by this equation, however. For this discussion, these techniques will be grouped into three main categories: (1) using the proper type of radiation to image the desired material (η_{Scint}, φ_N (η_{Target}, η_{Mod}, I_D), $\varepsilon_{Contrast}$, $e^{-\mu X}$), (2) modifications made to our specific experimental equipment (η_{Scint}, φ_N (η_{Target}, η_{Mod}, I_D)), (3) varying the time of exposure (t), and (4) varying the resolution,.

9.1. Optimizing the Neutron Energy (η_{Scint}, φ_N (η_{Target}, η_{Mod}, I_D), $\varepsilon_{Contrast}$, $e^{-\mu X}$)

It is important to select the proper type of radiation as discussed in section 1.1, page 10. For use with neutron radiography, the question of the proper form of radiation becomes a question of selecting the proper energy and strength of the neutron beam. The optimal neutron energy depends on four factors: the beam attenuation in the substrate material ($e^{-\mu X}$), the beam attenuation in the phantom material ($\varepsilon_{Contrast}$), the strength of the beam that can be produced at that energy (φ_N (η_{Target}, η_{Mod}, I_D)), and our ability to detect the neutron beam at that energy (η_{Scint}). An improvement in any or all of these factors will improve the signal to noise of the system.

A beam energy must be selected such that the substrate material will have the lowest attenuation of the neutron beam. Atoms have a strong energy dependence for which the chance of interaction with the beam will change by many orders of magnitude. Because the attenuation coefficient is highly dependent on the energy of the neutron beam, an energy should be selected which maximizes the product of the transmittance of the beam ($e^{-\mu X}$) if possible. The atomic make-up of the substrate material will determine how much of the beam is attenuated in the substrate. For example, the aluminum substrate which surrounds the corrosion attenuates only a small fraction of the neutron beam. A stronger beam would be required if the aluminum attenuated a significant portion of the incident neutrons.

The phantom, however, should attenuate the neutron beam very strongly. As defined earlier, a measure of how strongly the phantom (in our case hidden corrosion) attenuates the

beam is measured by the contrast effect ($\varepsilon_{Contrast}$) of the phantom. If the attenuation of the beam by the phantom is very high, the contrast effect approaches its theoretical maximum of unity. Like the substrate material, the attenuation of the phantom is highly dependent upon the neutron energy. However, unlike the substrate material, a neutron energy should be selected to maximize the attenuation due to the phantom (and thus maximize the contrast effect). If the material shows a high contrast, the contrast effect ($\varepsilon_{Contrast}$) would be very close to 1, and the signal to noise of the contrast would approximate the signal to noise of our system.

Therefore, selecting the proper beam energy is a critical part of neutron radiography. For an accelerator source, selecting the proper beam energy and strength also means selecting the proper combination of beam type, beam energy and target material. These parameters control the type and rate of the nuclear reaction that will take place. There are only a small number reactions we could reasonable use, which yield high percentages of mono-energetic neutrons.

We could attempt to alter the energy of the neutron after it has been produced through collisions in a process known as moderation. The nuclear reaction should be optimized with the proper moderator design to yield the desired neutron energy spectrum. However, this design goal has many limits. Moderation is an inefficient process, and it may not be possible to produce a strong enough source from an accelerator at many energies. In addition, the neutron beam from a moderator is often contaminated with a significant percentage of neutrons at undesired energies. The unwanted neutron energies can often be removed by filters made of materials that show a strong absorption at those energies. However it can be difficult to design a filter that will stop undesirable neutrons without attenuating, to some degree, the neutrons at the desired energy.

Once we have an beam of neutrons at the desired energy, we must be able to detect them with an efficient, high spacial resolution detector. This means that such a detector must exist at that neutron energy to yield the overall goal of the highest number of detected neutrons. This is a problem because there are a large number of energies for which such a detector is not available. In addition, the detector must be made to be insensitive to neutron energies outside our beam parameters. If this is not possible, a filter will have to be added to remove the neutrons of the undesirable energies.

It is possible to build a filter for removing unwanted neutron energies based on a time of flight method. This is only possible with a pulsed source in combination with an electronically gated detector (CCD or image intensifiers could be gated at the speeds required). This will be discussed in greater detail in chapter 10.

Creating and detecting a tailored neutron energy beam may be challenging. A very high contrast can be realized, however, by minimizing the substrate's attenuation of the beam and maximizing the phantom attenuation's of the beam. For example, sub-thermal neutrons may show a much higher interaction rate for some corrosion products than thermal neutrons. We could take advantage of this increase if we could create a tailored sub-thermal neutron beam (possibly by cooling the moderator). The art of creating and detecting a mono-energetic neutron beam to maximize the contrast and eliminate substrate attenuation is the basis upon which neutron resonance imaging relies. Neutron resonance imaging will be discussed in section 10.4.

9.2. Modifications to the Equipment (η_{Scint}, φ_N (η_{Target}, η_{Mod}, I_D))

Once we have selected the optimal neutron beam energy to use for our imaging system, we must customize our experimental setup to maximize the number of detected neutrons. There are many modifications that can be made to our equipment to improve neutron production, and thus increase the signal to noise.

9.2.1. Increased Neutron Production (η_{Target}, I_D)

One way to increase the neutron production is to increase the ion beam current delivered to the target. Another way would be to change the energy of the incident beam, and thus affect the kinetics of the nuclear reaction. Finally, we could select a more prolific neutron reaction, by changing one or both of the materials used as the ion beam material or target.

It is possible to increase the beam current to produce more neutrons. The number of neutrons produced is directly proportional to the deuteron beam place on the target. However, we are constrained by power limitations of the accelerator (2.25% duty cycle) and the thermal heating of our target. We could increase our power supply capabilities, and either run longer duty cycles or accelerate more particles during a pulse. The thermal heating of our target can be alleviated, to a certain extent, by cooling a stationary target. If the beam is depositing more energy than the target can remove by convection, conduction or radiation, than it is possible to using a moving target, such as a spinning target or a circulating gas. This will spread the heat input over a much larger area.

We could alter the energy of the incident beam to change the kinetics of the reaction to a regime where more neutrons thermal neutrons are produced at the detector area. For example, as was discussed in section 5.1.2, our experimental setup would benefit significantly by a deuteron beam energy increase of about 200 KeV. At that energy, the $^{9}Be(d,n)^{10}B$ reaction releases significantly more thermal neutrons. One method that has been investigated to give our incident beam the extra 200 KeV is to lower the target voltage to -200 KeV with respect to the ion production. This would accelerate the ion beam into the target at (900+200 KeV) = 1100 KeV.

Finally, we could alter the target to find a nuclear reaction that would produce more thermal neutrons at our detector area. For example, our gas target uses a deuterium gas to replace the standard beryllium target. The reaction $d(d,n)He^3$ will produce significantly more neutrons for the same incident beam.

Note that the goal is not necessarily to produce the most neutrons, but rather to produce an energy spectrum which will (after moderation) yield the highest thermal flux at our target. This means that we must take the neutron energy spectrum and angular distribution into account in our calculations. It is especially important to consider this information in the subsequent design of a moderator, if required.

9.2.2. Increased Efficiency in Neutron Moderation and Collimation (η_{Mod})

As discussed in section 3.4.3, moderator design is a very complicated issue, even for simple geometries. Computer simulated design is essential. We formulated a design plan for which uses multiple trials of a computer simulated Monte Carlo technique, MCNP, for calculating an optimized geometry.

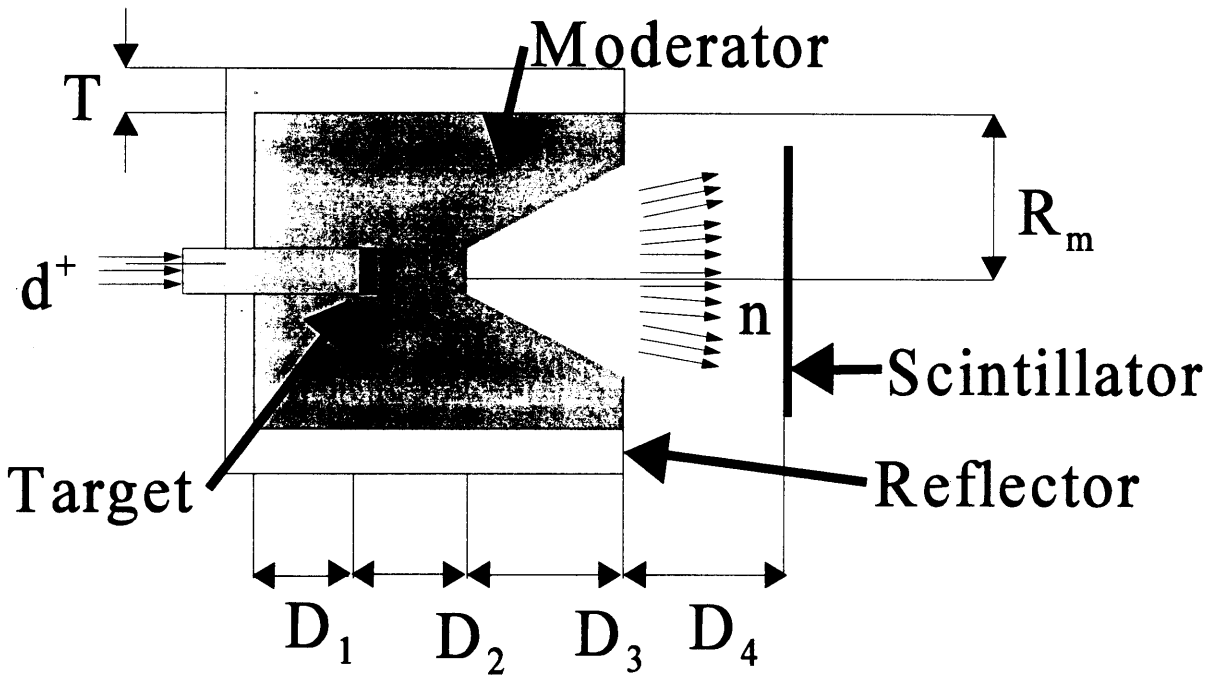

Figure 9.1: Optimizing Moderator/Collimator Design

Although a spherical geometry would be better, a cylindrical geometry was chosen to simplify the actual construction. As mentioned in section 3.4.3, a thin plate of heavy metal may be placed immediately after the target to quickly slow down fast neutrons. However, this was not incorporated into our model to help simplify our design, and reduce the number of parameters to be tested. The benefits of such a plate are questionable for our system which has a maximum neutron energy of less then 5 MeV. However, this assumption should be verified by simulation before a final design is manufactured.

The moderator design attempts to maximize the number of collimated thermal neutrons reaching the scintillator screen. Because we are imaging a relatively large area, we need a relatively large neutron beam. This requires a conical hole to made in the moderator to extract neutrons from our Thermal Neutron Peak (TMP) Position.

There are six main parameters to be tested: moderator radius (R_m), reflector thickness (T),

distance between back of moderator and the target (backspace distance- D_2), distance from target to TMP (D_2), distance from TMP to the front of the moderator (D_3), distance from the front of the moderator to the Scintillator Screen (D_4). It has been shown that an effective way to maximize thermal neutron production is to model the effects of each of these parameters independently, and choosing the best geometry from each of these.[20] Each variable will require between 5 and 10 different simulations to be able to maximize that parameter. The number of needed simulations grows linearly with the number of key variables.

There is a strong interdependence of each of the parameters. Optimizing the interactions between variables may yield significant gains. Unfortunately, to test these interactions, the number of needed simulations grows exponentially with the number of key variables. This made such an approach impractical due to computational limitations of running large numbers of MCNP simulations. One approach would be to use a simplified simulation code, a 2-D approach, and extrapolating the results to meet our needs. With the recent advancements in processing power of computers, it is possible to run multiple simulations on MCNP with much less computer time. To speed up the simulations, it is important that the MCNP runs be done with simple geometries.

A method has been developed to generate the input files for MCNP as we vary different parameters using Matlab software (The Math Works Inc, Prentice Hall, Inc.; Englewood Cliffs, NJ 07632). The input files can then be executed by MCNP and the results analyzed. The experimental setup initially uses a Box-Bacon multi-variable quadratic model to find local maxima and minima. This model requires ($3^k = 3^6 = 729$) independent MCNP trials. In addition, extra independent data sets will be have to be run to over-constrain our system and provide us information as to the error of our fit. Those variables which have been shown to not be accurately modeled by a quadratic equation will be re-evaluated and modeled either with a higher power equation, or another mathematical model such as an exponential.

From this model, the significance of each variable's interdependence can be studied. By removing from the model the statistically insignificant interdependence between variables, the model is greatly simplified and local minima and maxima can be remodeled using fewer MCNP trials.

If the moderator can not be effectively collimate the neutrons by itself, it is possible to collimate the neutron beam by passing it though many small tubes of length (L) and diameter (D). The ratio of L/D will determine the extent of collimation. It is necessary to have the beam collimated well-enough to not decrease the spatial resolution of the system, as discussed in section 4.4.

9.2.3. Increased Neutron Detection (η_{Scint})

It is possible to increase the number of neutrons detected by increasing the scintillator detection efficiency. As mentioned in section 1.3.1, page 32, there is a tradeoff between the detector efficiency and the gain (photons produced per neutron event detected). However, if

---

[20]Cluzeau, S. and P. Le Tourneur, "Upgrade of the Diane Performance".

using a lower gain scintillator screen does not affect our ability to remain quantum limited, we can afford to increase the detection efficiency at the expense of the gain. Even if we are not quantum limited, a lower gain scintillator screen may not degrade our signal from a detected neutron significantly. In this case, the higher detection efficiency of the screen will improve the signal to noise of the system. For example, we purchased a new scintillator screen with a 260% increase in detection efficiency which increased our signal to noise by 60%.

If the light output tradeoff is prohibitive, an intensifier can be used to boost the signal. As mentioned in the discussion about noise, such a device will contribute to the noise of the system and a calculation must be done to ensure the signal to noise of the system with the intensifier is better than the signal to noise of the original system. Another way to deal with the decreased light output is to alter the optical system by imaging a smaller area by moving the lens closer to the screen. This will have the double effect of decreasing the minification in the system and increasing percentage of light captured (η_Ω) until the system is quantum limited again.

9.3. Time of Exposure Tradeoffs (t)

A longer exposure time will yield a less noisy system. Aside from the practical time limitations of a particular experiment, the well depth of the CCD is finite, and will limit the total time of an exposure. Therefore, anything that will extend the depth of the CCD is useful.

One counter-intuitive result of this is that if we are truly quantum limited, it is possible to increase the S/N by decreasing the amount of light per event that reaches the CCD. This will allow longer exposure times before the CCD well is filled. This can be done with a lower scintillator gain, or a large optical loss. Obviously, we must be careful when we affect the signal in this manner to ensure that we do not decrease the S/N by increasing another source of noise that is dependent on that stronger signal. The light output should only be decreased while the system is still quantum limited. If the largest source of noise is still the statistical noise of the neutrons, then decreasing the strength of the signal reaching the CCD is a feasible way to accomplish a longer exposure time.

If the CCD well is filling up with an appreciable amount of dark current, the S/N could be improved by lowering the dark current rate (which would also decrease the dark current noise) and therefore filling the new dark current vacancy in the well with signal from a longer exposure time. This could be accomplished by purchasing a low noise CCD or by cooling the CCD to cut down the dark current rate. As discussed in chapter 5, our CCD camera can be cooled to -50°. Yet another way to get around the finite capacitor well size is to take multiple pictures, and then add the results off chip. This allows you to increase the signal, while the noise adds in quadrature. The signal to noise for such a system is different from the signal to noise calculated for our system. Therefore, a separate signal to noise calculation would have to be done. Kolbe, Turko and Berkely investigated methods of reducing the noise by averaging multiple short exposures in place of one long exposure.[21]

---

[21]Kolbe, Turko, Berkely, "Recovery of Very Low Intensity CCD Images From Noise", pp 731 - 733.

Many times, the exposure time is limited by other concerns, such as time constraints on the experiment. For example, the ability to reconstruct an object in a 3-D tomography technique depends very strongly on the number of pictures taken. If an individual exposure takes 5 minutes or longer, a tomographic reconstruction requiring 100 pictures would take over 8 hours. This is not a feasible option for many reasons. For these applications, increasing the S/N by taking longer exposures is not a solution.

9.4. Resolution Tradeoffs

It is possible to gain significantly better S/N by degrading the resolution. For example, by binning four pixels together, the aggregate signal strength is four times larger than each of the individual pixels. If the system is quantum limited, the S/N will have increased by a factor of 2. However, the area of a pixel has also increased by a factor of 4 which will decrease the resolution by an equal amount. Therefore, a much lower fluence is required for lower spatial resolution systems.

10. Recommendations and Conclusions

This research prompted a number of suggestions for future work. The following four major recommendations are discussed in the following sections:

-Use a quantum limited detection system for low fluence sources. The most effective method to a achieve this is by using a counting circuit.

-Increase the detected neutron fluence. The best methods will be through a better moderator design, increasing the beam energy to 1100 keV, and decreasing the required resolution when possible.

-Apply the counting circuit concepts to other fields that may benefit

-Investigate the possibility of using neutron energies other than thermal. This technique is known as neutron resonance imaging. Two areas of interest are using neutrons in the subthermal (<.025 eV) and epithermal (1-100 eV) range.

In addition to these suggestions, a number of observations have been made:

-It is possible to develop a CCD imaging system without using a cooled CCD camera

-It would be easy to apply this experimental setup to fast neutron radiography or x-ray radiography.

-Simultaneous data collection of multiple types of radiation may be convoluted to form a single enhanced image, and thus gain more information than one type of radiation can provide alone. For instance, x-rays (a by-product of an accelerator based neutron source) could be used to define features of the phantom that neutrons could not provide. Such a technique could be useful, even if only used to provide an image of macro features or edges that can be used as a relative reference frame.

-Moderation design, to date, has not adequately investigated the interdependence between variables. Moderator design may greatly benefit by a study which identifies and models the important covariance between parameter variables.

10.1. Recommended Detection System

The first finding of this report is that it is essential to our project that a quantum limited system be used. We would like to use a portable neutron accelerator source in place of the conventional reactor based source. The accelerator source produces a significantly lower neutron fluence than a reactor source. Therefore, it is vital that we use a very efficient neutron detection system for accelerator based neutron radiography. Of the investigated systems, the optimized system would be a bubble finding counter circuit based on a neutron scintillator screen system optically coupled to an intensified, a fast frame rate CCD.

A counting circuit offers the most potential for both eliminating detector noise and filtering unwanted detector response to other forms of radiation. The bubble finder circuit yields the highest spatial resolution, and offers yet another filter to remove system noise. The intensifier is necessary to boost the signal to noise of the system to a quantum limited system, rather than one that is limited by detector noise. For a pulsed neutron source, it also offers a way to remove noise based on time discrimination.

Development of this system is limited by the current technology of fast CCD cameras and the processing speed of today's computers. Although the technology is very rapidly increasing, it is now only feasible for low flux rates and small imaged areas, unless it is acceptable to post process the imaging data. If a high flux or large area is desired, currently the next best option would be a simple threshold circuit coupled based on the same scintillator screen - fast frame rate, intensified CCD system. The major disadvantage of this system is that it would have a spatial resolution at least two times lower than the scintillator screen ($> 2*100\ \mu m \approx 200\ \mu m$). If this resolution is not prohibitive, the simple thresholding system allows much higher fluxes and the computational requirements easily are within current technology, even at very high frame rates.

As mentioned in section 8.2, it is desirable to replace the CCD with cheaper, more capable technology. For example, CID detectors offer the potential to provide lower cost detection systems. A detector based on an amorphous silicon detector could very easily replace the bulky optical system and most likely would not require an intensifier.

10.2. Recommendations for Increasing Detected Neutron Fluence

It is desired to maximize the detected neutron fluence of our portable system. The best methods of doing this have been outlined in this paper: (1) increase the accelerator source strength, (2) increasing moderator/collimator efficiency, and (3) increasing the efficiency of the detector. Any incremental increase in any of these three factors will increase the system signal to noise.

10.3. Other Applications for Counting Circuits

Many applications, such as scattering experiments, could greatly benefit from a quantum limited, high spatial resolution, cheap neutron detection system. The counting circuit has the most potential for making a low cost quantum limited system investigated. Aside from its ability to desensitize our system to noise, the addition of a gated intensifier, or high frame rate CCD could be used to give the system an excellent time resolution as well.

10.4. Neutron Resonance Imaging with a Pulsed Neutron Source

As discussed in chapter 9, neutron resonance imaging could provide a much higher contrast than alternative methods. Our system, however, must be capable of producing and detecting enough of this neutrons at the desired energy to achieve a true improvement in our overall system signal to noise.

A time of flight method could be used to select specific neutron energies from a pulsed neutron accelerator source. Some neutrons will pass through the moderator unaffected, and strike the detector with no loss in kinetic energy. Others will suffer collisions in the moderator. A fraction of those that collide in the moderator will arrive at our detector some time later. The time delay is due to two factors- increased travel distance (flight path) and a slower velocity due

to loss of kinetic energy in the moderator.

Our system produces a spectrum of neutron energies at the detector. If we were to stand away from the target some distance (x), we would see neutrons ($mc^2 \approx 1$ GeV) with different energies (E_n) arrive at different times (t_n). Because our system does not produce any relativistic neutrons, the time of arrival is simply:

$$t_n = x\sqrt{\frac{m}{2\,E_n}} = \frac{x}{c}\sqrt{\frac{mc^2}{2\,E_n}} \qquad \textbf{(10.1)}$$

At a distance of 100 cm the first neutron of our system ($E_n < 5$ MeV), would arrive after a delay of 33 ns. This is the basis of time of flight neutron energy selection. The spacing between pulses has been exaggerated in the following diagram to emphasize the time of flight method. The differences in height between the pulse at the target and the pulse at the detector are due in part to $1/r^2$ losses: as the neutrons travel away from the target, their concentration per unit area decreases.

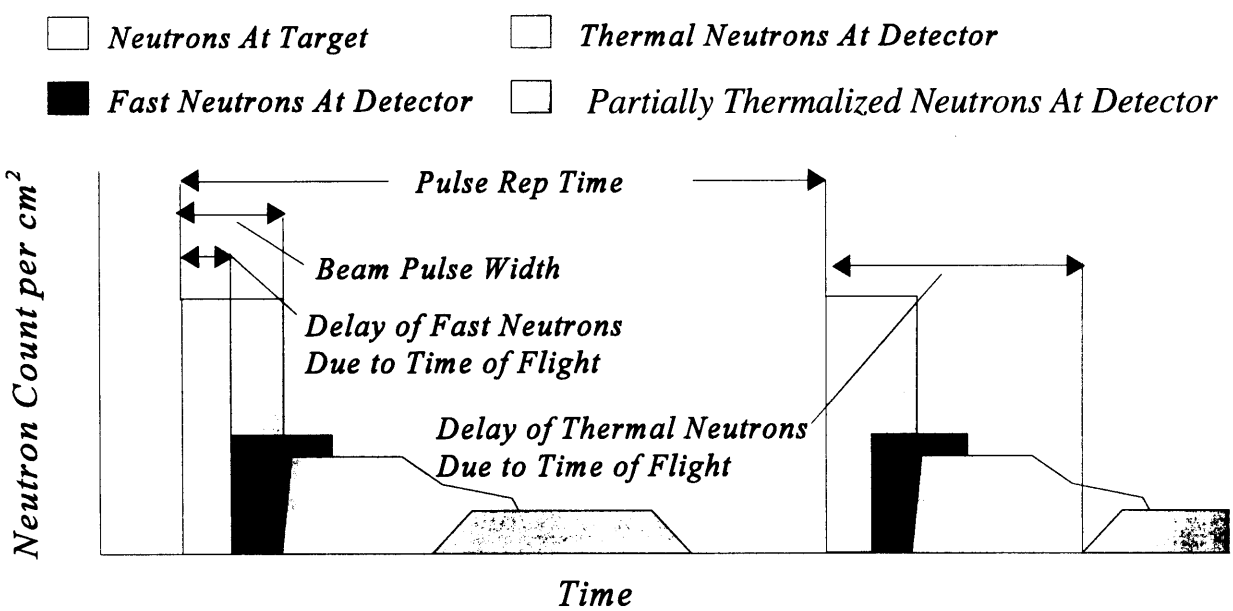

Figure 10.1: Delay of neutrons arriving at our detector due to time of flight

It would take a thermal neutron ($E \approx .025$ eV) 471 μs to travel the same distance. Of course, any neutrons that entered into a moderator to be thermalized would undergo a number of collision, and as a result, would have a longer flight path than our actual distance from the target. The flight paths and times could be estimated using a simulation such as MCNP.

The moderator will have the effect of spreading the pulse time of moderated neutrons at the detector. This will create a much longer pulse of moderated neutrons than the original pulse

of fast neutrons. To prevent the pulses of different energy neutrons from overlapping, it is important to start off with narrow pulses of deuteron on target. The ability to select specific energy bands will depend on a narrow (time) pulse of neutrons produced at the target.

Modern CCDs can be read within $t \geq 10$ ms, electronically shuttered within $t \geq 1$ ms, and cleaned within $t \geq 1$ μs. If a light intensifier were added to the system, it could be gated very quickly, within $t \geq 5$ ns. A CCD based system time of flight system can be used to gather a specific energy of neutrons.[22] To reduce overlap in times between energy groups, it is better to have a very narrow beam pulse width. To reduce overlap between pulses, it is important that the pulse repetition time be greater than the arrival time of the neutrons.

It is interesting to note that gamma radiation will see much less of a delay than our fastest neutron, because it travels at the speed of light. It is possible, therefore, to use the time of flight method to remove the response of both unwanted neutron energy spectrums, as well as gamma radiation.

It is also interesting that a CCD system could select specific energy bands of neutrons if the time resolution of the spectrum was well measured. Therefore we could in theory select any of the energy neutron our system is capable of producing to use it as our neutron energy. This is important because most isotopes show large resonance peaks (like the ones we saw in oxygen and aluminum in section 3.3). If we can select the energy neutron in the resonance region for a specific isotope s we would like to image with, we can realize very large contrast differences between that isotope and the material that surrounds it due these resonances. We would then be able to image practically any material inside of another.[23] This is known as neutron resonance imaging. In a sense, we are using neutron resonance imaging by thermalizing our neutron beam using a moderator in order to take advantage of the large differences in cross-section between $Al(OH)_3$ and Al.[24]

A relatively mono-energetic neutron source can be provided by running the neutron beam through a series of filters that absorb those neutrons from unwanted energy ranges.[25] This method can be quite inefficient for some beam energies. The combination of filters and a time of flight method may allow us to image with just about any energy neutron.

Neutron resonance imaging used in conjunction with a quantum limited detector would provide much higher contrast than alternative methods. However, the total signal to noise would depend, in large part, to the strength of the neutron beam that was produced and detected at the required energy. Thus, as discussed in chapter 9, the main difficulty to overcome is that we must be capable of producing and detecting enough of this energy neutron to get a reasonable

---

[22]Guzek, J., C. B. Franklyn, G. Pfister, M. C. Steyn, J. I. W Watterson, A. K. Schatz, and U. A. S. Tapper, The feasibility of Time-of-Flight Fast Neutron Radiography".

[23]Scrack, R. A., "NBS Work on Neutron Resonance Radiography", pp100-113

[24]Feiertag, T. H., "Thermal Neutron Radiograph at Los Alamos", pp 123-124.

[25]Stelts, Marion, and Bendt, P. J., "Neutron Resonance Filtering and Tests of Beam Quality", pp 116-118.

signal to noise. For example, if we attempt to use neutron resonance imaging to gain a contrast effect that increased by a factor of 20, we would have to ensure our S/N did not decrease by the same factor or more due to neutron statistical noise caused by a lower number of neutrons.

Neutron resonance imaging is one of many ways that the signal to noise in of a neutron radiography system could be improved.

Appendix: Listing of Variables

Parameter	Variable	Desired Effect	Limitations
Scintillator Detection Efficiency	η_{Scint}	Increase	Fraction of Detected Neutrons of Those Incident on Screen
Target Neutron Production Efficiency	η_{Target}	Increase	Beam Input Energy, Heating Limitations, Reaction Kinetics
Moderator and Collimator Efficiency	η_{Mod}	Increase	Size of Target Area, Design Limitations
Lens Solid Angle Efficiency	η_{Ω}	Increase	Optical Design Limitations
Lens Transmission Efficiency	η_{Lens}	Increase	Lens Absorption/Reflection Losses
Scintillator Fixed Pattern Noise	$\sigma_{Scint\ Pattern}$	Decrease	Uniformity of Manufacture Process
CCD Read Noise	$\sigma_{Read\ Noise}$	Decrease	CCD Technology Limited
Beam Current	I_D	Increase	Accelerator Design Limited
CCD Dark Current Collection Rate	K_{DC}	Decrease	Temperature of Camera, CCD Technology Limited
Exposure Time	t	Increase	Cost of Operating Time
CCD Photon to Electron Gain	G_{CCD}	Increase	CCD Technology Limited: Use Scintillator that Emits Red Light
Scintillator Detected Neutron to Photon Gain	G_{Scint}	Increase	Loss of Scintillator Detection Efficiency
Thermal Neutron Flux at the Scintillator Screen	φ_N	Increase	η_{Target}, η_{Mod}, I_D, Size of Scintillator Screen
CCD Response to Extraneous Radiation	$\sigma_{CCD\ Rad}$	Decrease	Shielding of CCD
Scintillator Cosmic Ray Response	$\sigma_{Cosmic\ Ray}$	Decrease	Shielding of CCD from Atmospheric Cosmic Rays
Scintillator Gamma Response	σ_{γ}	Decrease	Time of Flight Method to Remove Gamma Response

Contrast Effect	$\varepsilon_{Contrast}$	Increase	Constrained by Substrate and Corrosion Material and Energy and Type of Radiation Selected
Scintillator Fast Neutron Response	$\sigma_{Fast\ N}$	Decrease	Time of Flight Method to Remove Fast Neutrons

References:

Cluzeau, S., and P. Le Tourneur, "Upgrade of the Diane Performance", Fifth World Conference on Neutron Radiography, Berlin Germany, June 17-20, 1996.

DiCello, J.F., McCabe, C.W., Doss, J.D., and Paciotti, M. *The Relative Efficiency of Soft-Error Induction in 4K Static RAMs by Muons and Pions.* IEEE Transactions on Nuclear Science, Vol. NS-30, No. 6, December 1983. pp. 4613-4615.

DiCello, J.F., Paciotti, M. and Schillaci, M.E. *An Estimate of Error Rates in Integrated Circuits at Aircraft Altitudes and at Sea Level.* Nuclear Instruments and Methods in Physics Research B40/41. 1989. pp. 1295-1299.

DiCello, J.F., Schillaci, M.E., McCabe, C.W., Doss, J.D., Paciotti, M., and Berardo, P. *Meson Interactions in NMOS and CMOS Static RAMs.* IEEE Transactions on Nuclear Science. Vol. NS-32, No. 6, December 1985. pp. 4201-4205.

DiCello, J.F., Schillaci, M.E., and Liu, Lon-Chang. *Cross Sections for Pion, Proton, and Heavy Ion Production from 800 MeV Protons Incident Upon Aluminum and Silicon.* Nuclear Instruments and Methods in Physics Research. B45. 1990. pp. 135-138.

Feiertag, T. H., "Thermal Neutron Radiograph at Los Alamos", Neutron Resonance Radiography Workshop, Los Alamos, New Mexico, LA-11393-C Conference, UC-414, pp 123-124 (July 1988).

Fraser, G.W., "Thermal Neutron Imaging", International Workshop on High Energy Astronomy, Capri, Netherlands; Sept, 94.

Guzek, J, C. B. Franklyn, G. Pfister, M. C. Steyn, J. I. W. Watterson, A. K. Schatz, and U. A. S. Tapper, "The Feasibility of Time-of-Flight Fast Neutron Radiography", DeBeers Diamond Research Laboratory, P.O. Box 1770, SOUTHDALE, 2135, South Africa.

Iverson, Erik, "A Windowless Gas Target Accelerator", PhD Thesis, MIT Department of Nuclear Engineering, December 1996.

Kolbe, W. F. and B. T. Turko, "Recovery of Low Intensity CCD Images from Noise", IEEE Transactions on Nuclear Science, Vol. 36, No 1, February 1989. pp 731 - 733.

Lanza, Richard C. "The use of Neutron Tomographic Techniques for the Detection of Corrosion Damage in Aircraft Structures", ASME Winter Annual Meeting, Symposium on Structural Integrity in Aging Aircraft, 1995.

Lanza, R.C., E.W. McFarland and G.W. Poulus, "Computerized Neutron Tomography for Core Analysis", SCA Conference Paper Number 9128, 1991.

McFarland, Eric W., Hongli Dai, Helen Na, Richard Lanza, "Segmented Array Reconstructions for Tomographic Imaging of large Objects: Theory and Application to Neutron Computed Tomography" IEEE Transactions on Nuclear Science, vol 40, No 4, 1275 - 1281, August 1993.

Scrack, R.A., "NBS Work on Neutron Resonance Radiography", Neutron Resonance Radiography Workshop, Los Alamos, New Mexico, LA-11393-C Conference, UC-414, pp 100-115 (July, 1988)

Shi, Shuanghe, "An Accelerator-Based Neutron Imaging System and Its Application to Detection of Corrosion in Aircraft", PhD Thesis, MIT Department of Nuclear Engineering, April 28, 1995.

Shpetnyi, A.I. "Energy and Angular Distributions of Neutrons Emitted in the $^{9}Be(d,n)^{10}B$ Reaction", Soviet Physics, JETP, 5 No 3, 1957. pp 357-361.

Spowart, A.R., "Measurement of the Absolute Scintillation Efficiency of Granular and Glass Neutorn Scintillators", Nuclear Instruments and Methods 75, 1969. pp 35-42.

Spowart, A.R., "Measurement of the Gamma Sensitivity of Granular and Glass Neutron Scintillators and Films", Nuclear Instruments and Methods 82, 1970. pp 1-6.

Spowart, A.R., "Optimising Neutron Scintillators for Neutron Radiography", British Journal of NDT, 2-11, March 1989. pp 2-11.

Spector, Garry, Tom McCollum and A.R. Spowart, "Scintillator Fiber Optic Long Counter for Neutron Detection", Nuclear Instruments and Methods in Physics Research, A309, 1991. pp 303-317.

Stelts, Marion, and Bendt, P. J., "Neutron Resonance Filtering and Tests of Beam Quality", Neutron Resonance Radiography Workshop, Los Alamos, New Mexico, LA-11393-C Conference, UC-414, pp 116-118 (July, 1988).

Street, R.A. and S. Nelson, "Amorphous Silicon Sensor Arrays for Radiation Imaging", Material Research Society, Symposium Processing. Vol 192, 1990. pp 441- 452.

Street, R., Private Conversations.

Tsoulfanidis, Nicholas, Measurement and Detection of Radiation, Hemisphere Publishing Corporation, 1983.

Letaw, John R. and Normand, E. *"Guidelines for Predicting Single Event Upsets in Neutron*

Environments." IEEE Transactions on Nuclear Science. Vol. 38, No. 6; Dec 1991. pp. 1500-1505.

Watterson, J. I. W. and R.C. Lanza, "The Reaction $^{9}Be(d,n)^{10}B$ as a Source for Fast and Thermal Neutron Radiography". Schonland Research Center, Department of Physics, University of Witwatersrand, Johannesburg 2050, South Africa.

Watterson, J. I. W., R.C. Lanza, J. Guzek, U. A. S. Tapper, W. R. Murray, and E. Iverson, "The Small Deuteron Accelerator as a Source of Slow Neutrons", [1]Schonland Research Center, Department of Physics, University of Witwatersrand, Johannesburg 2050, South Africa.

Ziegler, J.F. *IBM Experiments in Soft Fails in Computer Electronics.* IBM Journal of Research and Development. May 1995.